



Review

Catalytic lignin valorisation by depolymerisation, hydrogenation, demethylation and hydrodeoxygenation: Mechanism, chemical reaction kinetics and transport phenomena

Tina Ročnik^{a,b}, Blaž Likozar^a, Edita Jasiukaitytė-Grojzdek^{a,*}, Miha Grilc^{a,b,*}

^a Department of Catalysis and Chemical Reaction Engineering, National Institute of Chemistry, Hajdrihova 19, 1001 Ljubljana, Slovenia

^b University of Nova Gorica, Vipavska 13, 5000 Nova Gorica, Slovenia



ARTICLE INFO

Keywords:

Lignin
Valorisation
Depolymerisation
Mechanism
Kinetic modelling
Transport phenomena

ABSTRACT

The lignin-to-chemicals valorisation has increased the interest of the scientific community in exploring the effective lignin depolymerisation. Lignin is the most abundant natural resource of aromatic components with a high potential to be converted into the various chemicals, thus increasing the level of an integrated biorefinery. This review focuses on lignin depolymerisation mechanism, chemical reaction kinetics and transport phenomena studies, recently introduced in the field of lignin chemistry to understand the reactivity of lignin macromolecule in two- or three-phase systems with a heterogeneous catalyst, liquid solvent and gaseous source. Lignin depolymerisation involves several parallel and sequential reactions of aryl-ether bond cleavage leading to a complex mixture of numerous depolymerised components. Theoretical and mathematical approaches for understanding and predicting catalytic parameters with the kinetic modelling are also discussed. The modelling approaches and kinetic data from various works in the literature has been thoroughly systematically reviewed, processed and consistently presented and benchmarked in graphical and tabular form. The aspects of modelling heat and mass transfer during lignin depolymerisation and upgrade has also been reported.

1. Introduction

The ideas and challenges for sustainable chemistry and technology aim to produce energy, fuel and chemicals in a more environmentally friendly way. Lignocellulosic biomass is a promising renewable resource, an alternative to fossil fuels with a potential for complete utilisation and combination of ecologic and economic incentives. On the other hand, lignin is an unwanted constituent in the pulp industry and at the same time a renewable raw material for aromatics. Industrial source of lignin, mainly kraft, has been estimated to 50–70 million tons annually whereas the structural features induced during lignin isolation is often diminishing its potential for upgrading to value-added chemicals. However, the research on lignin valorisation has evolved over the last two decades and has been focused on fuels, materials (e.g. polymers, formaldehyde or epoxy resins) and chemicals as major targets to replace their petroleum-based counterparts [1–3].

Engineering approaches developed to utilise the lignin, could be divided into the following three aspects: fractionation of lignocellulosic (LC) biomass, lignin depolymerisation (LD), and upgrading to the

platform chemicals [4,5]. The LD step is the most challenging, as it usually depends on the fractionation process, conditions, and plant source. Sustainable development of LD should focus on providing the most desirable aromatic components with high yield and selectivity for further valorisation into the target products [6]. With this in mind, the depolymerisation mechanism and kinetic modelling approaches have been investigated in the lignin chemistry research for potential use and implementation at the industrial level. The most straightforward reported LD pathway involves β -O-4 ether bond cleavage within the lignin macromolecule, the lignin modification, the removal of various functional groups (carbonyl, methyl, and hydroxyl), and condensation (repolymerisation) reactions due to the formation of reactive hydroxyl radicals [4,7].

Kinetic modelling requires specific knowledge, but provides important insight into the behaviour of lignin in the reaction medium with respect to the solvent, catalyst, and the reactor used. Kinetic models aim to describe two- or three-phase systems, including the reaction kinetics, transport phenomena, and thermodynamics, to link experimental data with the theoretical domain [8]. During the depolymerisation lignin is

* Corresponding authors at: Department of Catalysis and Chemical Reaction Engineering, National Institute of Chemistry, Ljubljana, Slovenia.

E-mail addresses: edita.jasiukaityte@ki.si (E. Jasiukaitytė-Grojzdek), miha.grilc@ki.si (M. Grilc).

<https://doi.org/10.1016/j.cej.2022.137309>

Received 1 April 2022; Received in revised form 19 May 2022; Accepted 29 May 2022

Available online 31 May 2022

1385-8947/© 2022 The Author(s). Published by Elsevier B.V. This is an open access article under the CC BY license (<http://creativecommons.org/licenses/by/4.0/>).

transformed into different products. By applying frequently used lumped-model approach, products with a similar structural features are grouped into kinetic lumps to simplify the kinetic model, which allows definition of the kinetic parameters for specific depolymerisation steps [9].

On the other hand, studies on transport phenomena showed promising perspective for the optimisation of the chemical process as well as mass and diffusion limitations for batch or flow-through reactor types depending on the catalyst size. A third reactor type to examine LD reactions is the microreactor, especially beneficial due to its dimensions and the use of smaller catalyst particles eliminating diffusion limitations, which may not be suitable for the lab-scale reactors (up to 300 mL) [10].

Recent reviews [2,5,6,11–13] have highlighted the current developments regarding LD methods and conversion into various bio-based products. This review outlines the published LD mechanisms, kinetic parameters, and transport phenomena studies under the mild reaction conditions. The emphasis is given explicitly on lignin, excluding the studies made with lignin monomeric and dimeric model compounds.

2. Lignocellulosic biomass and lignin structure

Lignocellulosic (LC) biomass is composed of cellulose, lignin, and hemicellulose which are the major components of hardwood, softwood, and herbaceous plants. Cellulose is the most abundant renewable resource on earth that can be fully utilised in biorefinery processes, bioenergy, or in the chemical industry [5], while the majority of the lignin, is used as a high calorific value-energy source on site of the pulp and paper industry mainly because of the challenging utilisation of this complex natural aromatic polymer. Numerous studies have recognized lignin as a promising source of low molecular weight aromatic building blocks for high value applications [5,11]. Here, the high oxygen content in lignin can be a useful feature for the production of chemicals, but a disadvantage for biofuels [14].

Lignin content, structure, distribution of the monomeric units within, and the amount of methoxy groups depend greatly on the type and taxonomy of the plant, and additionally on the lignin isolation methodology [12,15]. Hardwoods contain 16–24 wt% of lignin composed of guaiacyl (G) and syringyl (S) units, softwoods – from 25 to 31 wt% of lignin which is structured from G-units only, while in grasses

the presence of 16–21 wt% of lignin composed of all three monolignols is confirmed [5,11]. Lignin consists of a randomized network of phenylpropane units linked by C-O or C-C bonds (Fig. 1) [5,12,16–18]. The common C-O bonds, such as β -O-4, α -O-4, and 4-O-5, in lignin are linked either as ethers or as part of a furan ring. In native lignin more than 45 % are β -O-4 ether bonds and 12 % are β -5 phenylcoumaran bonds [5,12,17]. The typical β -O-4 linkages in native lignin are also classified as A-type β -O-4 linkages ($\text{OH}_\alpha + \text{OH}_\gamma$ group), but B-type β -O-4 linkages consisting of β -O-4 motifs without a γ -carbinol group (OH_α group) are frequently present in technical lignins [19]. It is believed that the B-type of β -O-4 motif, which is more commonly identified as α -O-4 motif, is more accessible and easily cleaved during depolymerisation processes [5]. On the other hand, lignin also contains more recalcitrant C-C bonds present in dibenzodioxocin and biphenyl (5-5), phenylcoumaran (β -5), spirodienone (β -1), and resinol (β - β) structures [5,12].

The amount of C-C bonds in native lignin is related to the distribution of monomeric units (hydroxycinnamyl alcohols) called monolignols: *p*-coumaryl (H-unit), coniferyl (G-unit) and sinapyl (S-unit) alcohols (Fig. 1) [5,11,20]. The three hydroxycinnamyl alcohol monomers differ in their degree of methoxylation, showing how many methoxy groups are attached to the individual monolignol moiety [12,20], specifically: *p*-coumaryl alcohol has no methoxy groups, sinapyl alcohol has two, and coniferyl alcohol has one methoxy group [17]. In addition to methoxy groups, the structure of lignin also contains other functional groups, mainly phenolic and aliphatic hydroxyl, carboxyl and carbonyl groups. Aliphatic hydroxyl and carbonyl groups are associated with the lignin structure as substituents between the inter-units, while the methoxy and phenolic hydroxyl groups are a part of the lignin end-units [21]. The Van Krevelen diagram built by plotting the proportion of hydrogen-carbon and oxygen-carbon atomic ratio of more than 10 lignins, confirmed that hardwood lignin, which is mainly composed of G- and S-units, contains a lower amount of carbon and C-C type bonds than softwood lignin, which is mainly composed of only G-units [20]. Those particular structural differences additionally affect the depolymerisation temperature and solid residue formation as the higher reaction temperature is required for C-C bond cleavage (bond-dissociation energy up to 525 kJ mol^{-1}). Study with the softwood and hardwood lignin emphasized that the softwood lignin formed more solid residue than hardwood at $250 \text{ }^\circ\text{C}$ which accordingly was reduced at the increased process temperature ($285 \text{ }^\circ\text{C}$) [22].

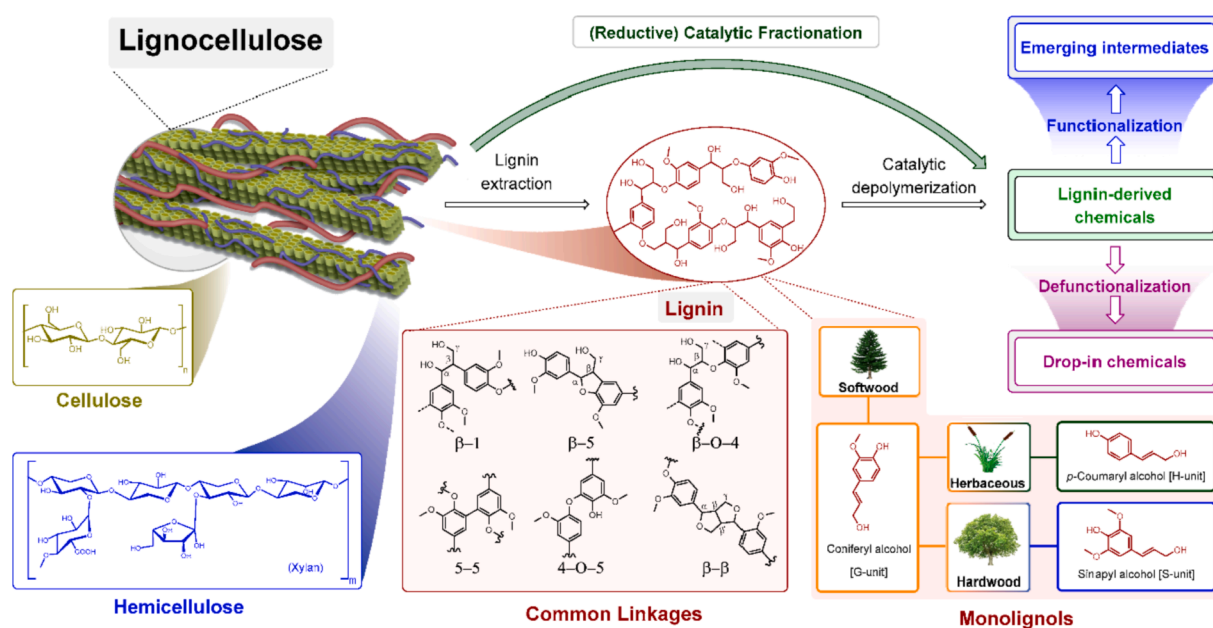


Fig. 1. Schematic representation of lignocellulosic biomass, lignin structure with the main building blocks and bond types, and possibilities for industrial implications. Republished with permission of MDPI from Korányi et al. [23].

In addition, lignin structure strongly depends on the type of the biomass pretreatment/lignin isolation procedure. Most commonly used processes in pulp and paper industry are kraft and soda [11,12,24] also known significantly to alter the lignin structure [6]. During the kraft process, the lignin is affected by sodium hydroxide and sodium sulphide where beside the increase of the phenolic hydroxyl group content, a considerable amount of sulphur is covalently bonded to the lignin in the form of thiols [11]. On the other hand, the soda pulping process is a sulphur-free method using the base as a catalyst and commonly applied for non-woody biomass (grass, straw, sugarcane bagasse, etc.) producing lignin with less contaminants [11,12]. Although, it has been estimated that only 10–15 % of lignin recovered from industrial source can be isolated without negatively affecting chemical structure. Another methods used for lignin extraction are sulphite, producing liginosulphonate lignin, ionic liquid-assisted biomass fractionation and organic solvent-assisted biomass hydrolysis producing organosolv lignin etc. [5,11,12,17,25,26].

During the environmentally friendly organosolv lignin extraction, an aqueous organic solvent with organic/mineral acids (H_2SO_4 , HCl, acetic acid, formic acid or peroxyorganic acids) is used to catalyse the hydrolysis reaction [24]. During the pretreatment, mainly lignin-carbohydrate and α -O-4 bonds in the lignin are broken to separate it from the LC biomass [11]. The organosolv process, especially at mild reaction conditions, has been recognized as an efficient way to preserve the native lignin structure, which is rich in β -O-4 ether bonds [6,12].

Implementation of the alternative lignin isolation techniques promoted biomass fractionation under mild processing conditions producing β -O-4 rich and less condensed lignin, however with the limited yields up to 20 % relative to the total weight of LC biomass starting material [4,27]. The content of easily cleavable β -O-4 bonds strongly affects the degree of catalytic LD. Additionally, lignin structure and its extraction processes have been described in detail by other authors in several review articles [5,6,11–13].

3. Lignin depolymerisation mechanisms

Depolymerisation of lignin is an outcome of a several simultaneous reactions, specifically: cleavage of the inter-unit bonds (modification of lignin structure), defunctionalisation (decarboxylation, demethylation), hydrodeoxygenation (HDO), and crosslinking reactions [7] and proceeds according to the specific reaction mechanisms depending on the process conditions (acidic, basic, oxidative, reductive).

Inter-unit linkages within the lignin macromolecule have different bond-dissociation energies (BDEs) which was determined within a comprehensive study using more than 65 different lignin model compounds with C-O (α -O-4, β -O-4, 4-O-5) and C-C (β -1, 5-5, β -5) bonds. Average BDEs of examined model compounds (in Fig. 2) clearly indicates C-O bonds to be more susceptible to depolymerisation, while more forcing reaction conditions are required for the C-C bond scission [5,28,29].

Ether (α -O-4, β -O-4) are the weakest linkages in the lignin matrix and are predominantly broken during LD [24], while the influence of the substituents and their location on the aromatic rings could be foreseen due to a strong correlation between the strengths and bond distances [11,28]. A number of β -O-4 bonds in lignin therefore plays very important role as lignin conversion into the monomeric substituents proceeds specifically by cleaving β -O-4 bonds thus it is also used to calculate the theoretical maximum monomer yield of lignin [23,30]. The experimental monomer yield could be additionally affected by i) modifying the neighbouring functional groups and consequently lowering the β -O-4 linkage BDE (Fig. 3) [31], ii) increasing the polarity of solvent [24,30], while the overall lignin conversion into monoaromatics additionally depends on the type of biomass, the intrinsic ratio between the C-O and the C-C bonds, lignin isolation and depolymerisation methods, catalyst and solvent used for the depolymerisation [5,15,17,30]. Especially due to the lignin structural variability [5,6,12],

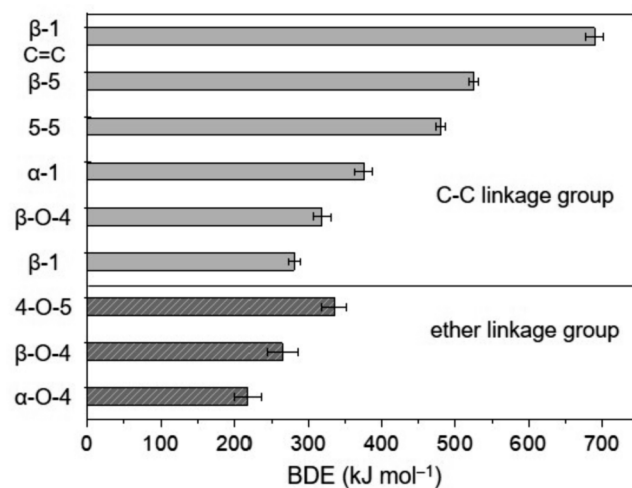


Fig. 2. Average bond-dissociation energies (BDEs) of lignin model compounds with C-O and C-C linkage groups. Reprinted with permission from Parthasarathi et al. [28] (BDE values were recalculated to kJ mol^{-1}).

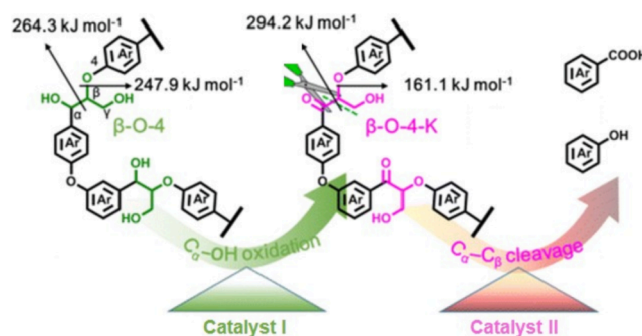


Fig. 3. Effect of neighbouring functional groups on BDE of β -O-4 bond. Reprinted with permission from Wang et al. [31].

the development of the universal depolymerisation methodology, for instance synthesis of a general catalyst for selective C-O bond cleavage additionally preventing crosslinking reactions is a very challenging task [17].

LD pathway is composed of several parallel and sequential reactions through various mechanisms of hydrogenation, HDO, and dealkylation yielding smaller lignin fragments (oligomers) and phenolic components with reactive (hydroxyl) functional groups [16]. The accurate prediction of the reaction order with the detailed structure of components is extremely demanding due to the lack of information about the reaction intermediates (structure of the oligomeric units), the unknown position of the β -ether cleavage (through end- or inter-units), and the recalcitrant residue formation (through oligo- or monomeric units), etc. is required for the kinetic model development to describe the entire lignin depolymerisation.

Recent advances in the catalytic lignin conversion into the value-added monoaromatics are well reviewed and discussed elsewhere [2,5,6,12,16,17,32]. For the better understanding of the catalytic LD mechanism and kinetic parameters, key process characteristics about catalytic LD will be overviewed here. The main focus will be given on lignin modification specifics, its reactivity and β -ether bond cleavage that are further essential for comprehension of the LD mechanism and (micro)kinetics.

Lignin depolymerisation products and yields depend on the methodology applied, for instance a base- or acid-catalysed, reductive, oxidative, or thermal degradation process, as lignin structure is modified via simultaneous depolymerisation and condensation reactions [5,17].

3.1. Acid-catalysed mechanism

The acid-catalysed mechanism of the β -O-4 bond cleavage is shown in Scheme 1. Firstly, dehydration of the hydroxyl group at the C_{α} -position occurs which is followed by the subsequent formation of the quinone methide intermediate on the aliphatic chain side thus generating the corresponding Hibbert-type ketone. Since ketones are not formed in the significant amount, their loss was described as equilibrium to its enol ether-type form and further dehydration of the hydroxyl functional group. Afterwards, the β -aryl ether bond is reductively cleaved via an allylic rearrangement and the obtained intermediates are hydrogenated to monomeric ketone and phenol structures [33–35].

In lignin the reactivity of the β -O-4 bonds as well as the formation of the carbocation/quinone methide intermediates (involved in the cleavage mechanism of β -ethers) additionally differs depending on the type of the β -ether unit (free phenolic or an etherified phenolic) especially in alkaline media. The phenolic units are willingly converted into quinone methide transferring electronic features of the functional group to the carbon atom while the etherified phenolic units form quinone methide intermediates only in acidic environment [36].

Non-cyclic α -O-4-type and β -O-4 bonds cleavage followed by formation of the Hibbert-type ketone and enol ether linkage results in the loss of an aliphatic hydroxyl group, a carbon atom, and the formation of a phenolic hydroxyl group, while the cyclic α -aryl ethers, typically in phenylcoumaran, dialkyl ether and/or resinol structures are more difficult to depolymerise [33]. However, if the reactive carbocation intermediate is formed at the C_{α} -position, there is a possibility of stable C–C bond formation leading to the condensation reactions, unless the reactive site is stabilized with nucleophiles (MeOH, EtOH), which are known to successfully suppress the lignin repolymerisation [33,37].

3.2. Base-catalysed mechanism

The base-catalysed LD in presence of soluble (NaOH, KOH, etc.) or solid (MgO, CaO, etc.) bases generates phenolic units, which are more readily depolymerised compared to non-phenolic units where β -O-4 bond cleavage is relatively slow. During the base-catalysed LD phenolic monomers are primarily formed, while oligomeric units are the result of repolymerisation between the reactive species. Furthermore, the isolation of lignin monomeric units is strongly favoured in basic solution and proportional to base (e.g. NaOH) concentration [5,17,38]. In contrast to the base-catalysed, during the acid-catalysed LD, repolymerisation may occur either before or after the β -ether bonds cleavage [37] while a variety of Lewis (MCl_x , $M(OTf)_x$; M: Ni, Fe, Al, Cu, etc.) or Brønsted acids (H_2SO_4 , HCl, H_3PO_4 , HOTf, acidic zeolites, etc.) have been applied for this cleavage [5].

3.3. Reductive conditions

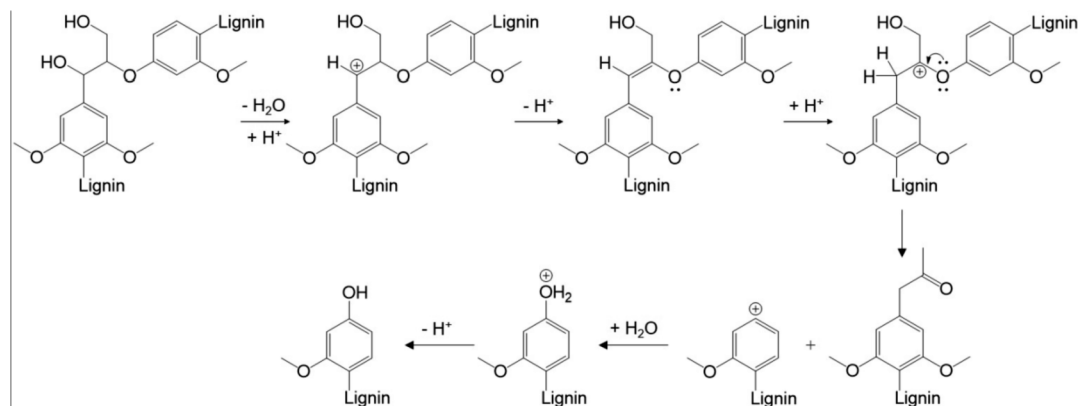
Various radical intermediates with the different reactivity and stability are formed during the reductive β -O-4 bond cleavage within the hydrogenation. Alkyl and phenoxy radicals are less reactive than hydroxyl radicals [39]. Nevertheless, under the reductive conditions, the β -O-4 is cleaved after the initial radical formation at the C_{α} -position. The release of the hydroxyl radical in the form of water molecule promotes the formation of the coniferyl alcohols and dihydroxybenzenes during the hydrogenation [40].

Lignin hydrotreatment has been frequently explored for an efficient LD approach [5,6]. Mild hydroprocessing reaction types modifying lignin macromolecule are dehydration, hydrocracking, hydrogenation, and HDO. The reaction conditions usually required for the mild hydroprocess are temperatures below 300 °C under higher hydrogen or inert atmosphere (3–12.5 MPa) while specific applied conditions depend on the use of the (noble or transition metal) catalysts [17]. The cleavage of the C–O linkage is usually attained by HDO and hydrogenation over heterogeneous catalysts with the elimination of oxygen, producing water as a by-product [5,16]. A metal catalyst with hydrogen gas or a H-donor solvent is required to cleave ether bonds and to remove OH_{α} , OH_{γ} and phenolic OH groups [19,23,41,42]. During the hydrotreatment, lignin is dissolved within the initial heating before reaching the catalyst activation temperature and proceeding further with the lignin conversion into oligo-, di- and monomeric fragments [4]. The activity of the transition metal catalysts could be reduced by the impurities depositing on the surface and it is especially significant during the kraft lignin depolymerisation [43]. The overview of the reductive LD is shown in Fig. 4, highlighting the attainable products, reaction conditions, the catalysts for the selective conversion into monomeric products with the maximum reported yields for each biomass type [5].

Recently, an increased attention is given to the reductive catalytic fractionation (RCF) strategy due to the efficient lignin conversion into desired products. RCF approach involves lignin extraction, depolymerisation and stabilisation [4,32,44,45]. The RCF process typically employs polar/protic solvent, a heterogeneous redox catalyst, and a reducing agent (pressurised hydrogen, an external or internal hydrogen donor) in the temperature range between 200 and 250 °C. A heterogeneous catalyst stabilises the formed unstable species and additionally affects LD via the hydrogenolysis of the aryl-ether bonds. Typically, the produced black liquor contains low-molecular weight oligomers, dimers, and monophenolics such as 4-n-propylguaiacol/-syringol, and 4-n-propenylguaiacol/-syringol [32].

3.4. Oxidative conditions

There are three main approaches of the oxidative LD which proceeds through the inter-unit bond cleavage, the aliphatic side-chain oxidative



Scheme 1. Mechanism of the acid-catalysed beta-aryl ether bond cleavage.

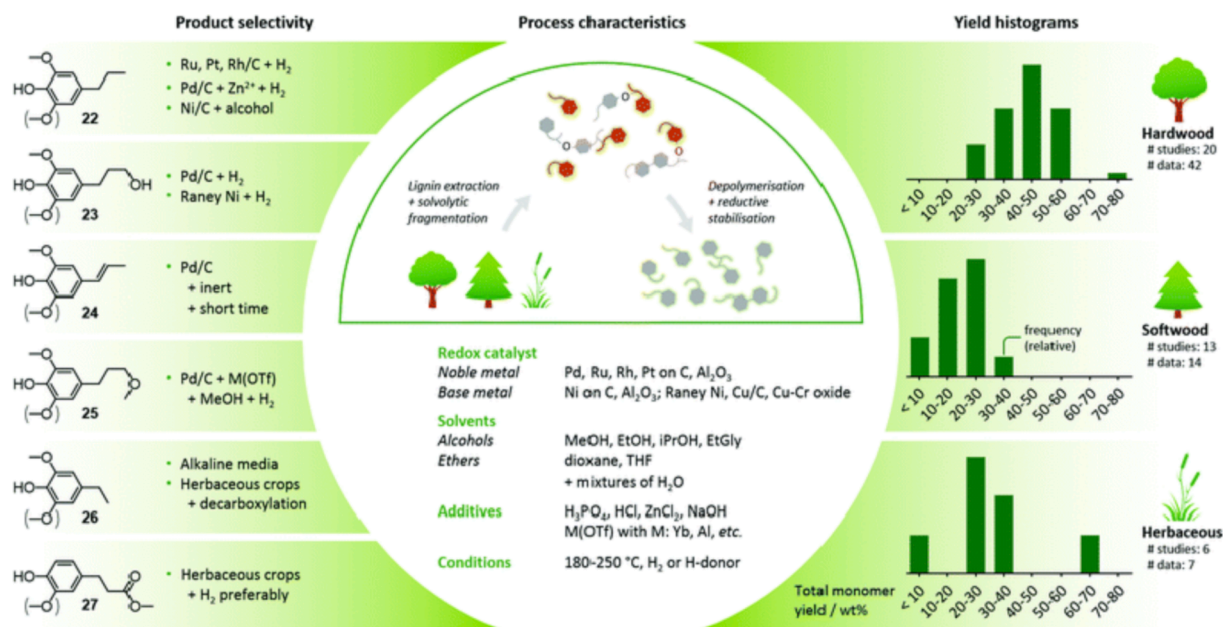
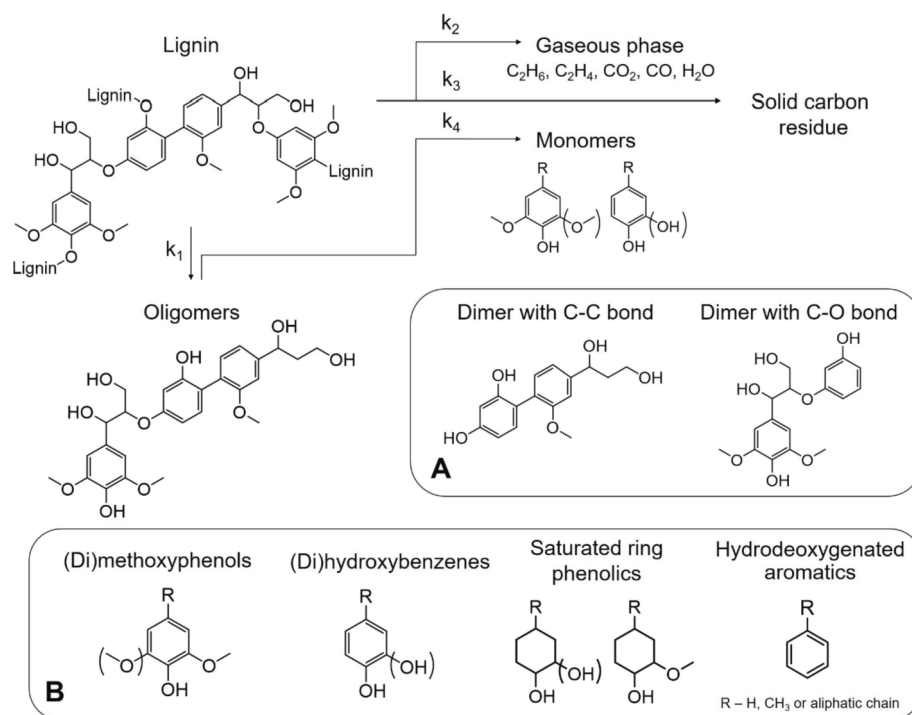


Fig. 4. Overview of lignin depolymerisation under reductive conditions. Republished with permission of Royal Society of Chemistry from Schutyser et al. [5].

modification and aromatic ring oxidation and ring cleavage reactions introducing more oxygen-containing functional groups (aldehydes, ketones, carboxyls) into the partially depolymerized lignin structure [46]. Most oxidative pathways are initiated by electrophilic reactions at positions of high electron density (*ortho*, *para*, or C₆) in lignin and proceed rather through the cleavage of the C–C linkage than the C–O bond. Oxidative processes may not be ideal solution due to the radical formation leading to the rapid repolymerisation of phenolic products, which are usually not stable in such oxidative reaction medium [5,17].

3.5. Process-dependent initial depolymerisation mechanisms

Although lignin structure is more complex than the one of model compounds, the tendencies of the typical bonds cleavage in model compounds are comparable to the ones in lignin. It is believed that LD can proceed through three main routes such as direct deoxygenation, hydrogenation and tautomerisation [16]. The direct C–O bond hydrogenolysis removes oxygenated functional groups leaving defunctionalised aromatic rings. However, since the hydrogenation reaction requires a lower temperature and higher pressure than hydrogenolysis, the cycloalkenes and cycloalkanes are expected due to the higher external



Scheme 2. LD pathway forming four main product groups (oligomers, monomers, gases, and solid carbon residue – ‘char’). A: dimeric intermediates, B: groups of monomeric products.

hydrogen supply [16,47].

In order to accelerate LD, many studies were performed and numerous catalysts were examined defining their activity/selectivity as outlined in Fig. 4 [5]. Metal catalysts, acid- and base-based catalysts effectively promoted β -O-4 bonds cleavage by reducing their activation energy [48,49]. However, it was found that the depolymerisation mechanisms differ giving a rise to various intermediates regardless the used catalyst [2,21,50]. The catalyst activity and selectivity screening studies performed using monomeric and dimeric model compounds are less complex and thus provide important insights about the catalyst suitability for LD [51].

The reaction mechanisms showing the complexity of the tentative pathways within the LD, were postulated based on experimental results depending on the research scope [9,39,52–54]. The initial LD mechanism can be presented as shown in Scheme 2, where the oligomers, monomers, gases and solid carbon residue ‘char’ are formed from lignin. Lignin-derived monomers probably occur after the cleavage of the C-O or C-C inter-unit linkages as intermediates (Scheme 2A). Further, the monomers obtained can be grouped regarding their substituents or degree of unsaturation (Scheme 2B). The more complex the reaction mechanism is, more variables need to be considered as options for the formation of oligo-/di-/monomers and gaseous products.

3.6. Monomer formation

Lignin is composed from the monomeric units interconnected through the linkages with different BDEs. The higher is the BDE, more challenging is to cleave a particular bond under the mild depolymerisation conditions. In general, the monomer yield strongly depends on the amount of the easily cleavable β -O-4 bonds in lignin. For example, if the trimer maintains only one ether bond (C-O), a dimer and a monomer will be formed, while the further dimer conversion into monomers is unlikely to proceed because of the highly recalcitrant C-C bond. In contrary, if the oligomer is composed of the monomeric units connected via β -O-4 linkages, the complete depolymerisation will be achieved [11]. However, it was proposed that the monomers (reactive radicals) produced during the depolymerisation, are the main units participating in the formation of the recalcitrant condensed structures which accordingly reduces monomer yields [39,52,55].

An efficient oxidative process to cleave C-C bonds was proposed by Dong et al. [56]. Authors have examined biphenyl 5–5 bond lignin model compounds under the oxidative conditions with multifunctional Ru/NbOPO₄ catalyst thus reporting conversions of diphenylmethane up to 58.5 % and diphenylethane up to 35.4 %. Evidently, monomer yields could additionally be increased by coupling the selective C-C bonds cleavage with LD methodology. Furthermore, the various (solid) acid-catalysed dealkylations of lignin monomeric components (C-C bond cleavage in side-chains) have been reported although the scissor of the C-C bonds in side-chains is accompanied by the C-O bond cleavage during LD [57].

Catalytic and non-catalytic LD proceeds differently. For instance, it was found that the depolymerisation of the dimeric model component progressed via a dissimilar intermediate in the absence of catalyst than in the presence of a noble or transition metal catalyst [21,30]. Li et al. [21] used guaiacyl-glycerol-beta-guaiacyl ether (GG) as a dimeric lignin end-unit component and found the non-catalytic reaction to proceed via a quinone methide intermediate to coniferyl alcohol and guaiacol, wherein the reaction to guaiacol being more dominant than the one to coniferyl alcohol. The comparison of the lignin end- and inter-unit non-catalytic pathways disclosed that only lignin end-units were involved in the reaction. In addition, hydrogenolysis of the lignin end-unit (model compound) was found to be up to 2.3 times faster over Pd/C catalyst than for internally bounded dimer, while both model compounds exhibited at least 90 % selectivity for dihydroconiferyl alcohol from the GG dimer and dihydroveratryl alcohol from the veratrylglycerol-beta-guaiacyl ether (VG). The reported activation energy for non-catalytic

reaction of lignin end-units was 98 kJ mol⁻¹ while the energy barriers for the catalytic cleavage of GG (end-unit; 72 kJ mol⁻¹) and VG (inter-unit; 78 kJ mol⁻¹) were rather similar, however pointing out the effect of the transition metal catalyst to reduce the activation energy for β -O-4 bond cleavage. It appears that lignin hydrogenolysis, hydrogenation, and consequently depolymerisation predominantly occurs at the end-units of the macromolecule [21].

3.6.1. Demethylation and demethoxylation

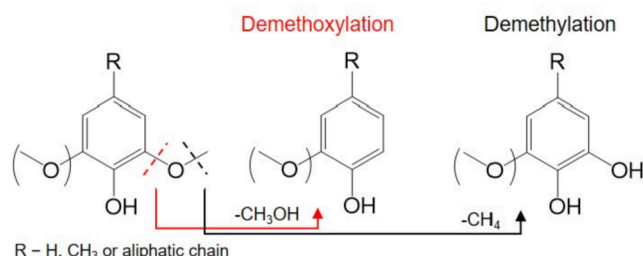
The dimer conversion into monomers produces single mono- or disubstituted aromatic rings with methoxy groups. After the depolymerisation of the hardwood lignin, dimethoxyphenols and methoxyphenols can be expected as intermediates if the primary lignin structure consists of G- and S-units, whereas in case of softwood LD only methoxyphenols can be expected. In case of herbaceous lignin, dimers can be converted into alkylphenols and (di)methoxyphenols, because all three monolignols are present. Otherwise, alkylphenols are obtained only after demethoxylation and HDO of the methoxylated phenols [9,53,58].

Further defunctionalisation of the (di)methoxyphenols can be carried out by demethoxylation and demethylation removing the methoxy or methyl groups, respectively. By replacing the methyl group with a hydrogen atom and depending on the initial degree of phenol methoxylation, various di- or trihydroxybenzene isomers are formed [7,9]. It is well known that the methyl and methoxy groups have the lowest BDE among the functional groups attached to the aromatic ring owing to the conjugative effect with oxygen atom [9,57], and therefore are the most susceptible to changes under reductive conditions. It certainly can be stated that methoxyphenols are converted via demethylation to catechols, and via demethoxylation to alkylphenols (Scheme 3) where the kinetic constants for both reactions are nearly equal [53,58]. Based on the studies performed with the lignin model compounds, the significant differences between demeth(ox)ylation reaction mechanisms were observed depending on the catalysis with non-promoted or promoted catalyst. For instance, the demethylation reaction was preferred in case of a non-promoted catalyst, while both the demethylation and demethoxylation transpired with promoted catalyst [59]. In addition, the demethylation was favored upon the use of the acidic support or catalyst with metal sulphide acid sites [59,60].

3.6.2. Hydrogenation and hydrodeoxygenation (HDO) of aromatic ring

In the presence of the noble/transition catalyst and a gaseous/external hydrogen, saturation/HDO of the benzene ring could be initiated [61]. The HDO of the phenolic monomers resulted in the removal of the hydroxyl group from either the aromatic or hydroxylated alkyl sites forming water as a by-product. The HDO and hydrogenation reactions followed two parallel pathways, whereby the phenolic monomer may be hydrodeoxygenated to a more stable benzene or saturated to cyclohexanol. However, the removal of the hydroxyl group from (alkyl) phenols is more challenging without the saturation of the aromatic ring [9]. Cyclohexanols can also be further hydrodeoxygenated to cycloalkanes, and even further to the cyclic alkanes [54,61].

A study with a lignin model component suggested that the rate



Scheme 3. Demethoxylation and demethylation of lignin model compound.

constants of removal of the methoxy and OH groups from the aromatic ring are 36- and 42-fold higher, respectively, compared to the rate constants for the saturated ring. It was confirmed that the activation energies for HDO were significantly higher for saturated reactants than for the unsaturated ones, while demethoxylation reactions showed more feasibility compared to dihydroxylation [8].

The comparison of the calculated LD kinetic parameters (rate constants) revealed HDO reaction to be slower than the gasification and repolymerisation, noting that the latter occurred via oxidised molecules such as catechols [53]. On the other hand, in the latest study it was pointed out, that the rate constant of the catechol conversion into phenol was higher than the rate constant of the condensation into solid residue [58]. Furthermore, Pu *et al.* [9] disclosed the aliphatic OH group dehydration to have highest reaction rate constant during LD, while the HDO of aromatic OH groups was the slowest reaction (the lowest rate constant) without using any catalyst in supercritical water. Therefore, it could be concluded that the aromatic OH groups were more stable thus requiring specific conditions for their removal compared to aliphatic OH, methyl or methoxy functional groups [58].

3.7. Solid carbon residue (char) formation

The formation of the highly condensed solid carbon residue so-called char is a result of the cross-linking between the reactive fragments formed during the reaction [52]. Cross-linking reactions occur when a substituent groups have been eliminated and two carbon sites are more favourable for bonding [7]. Two types of char can be formed during the LD: aromatic and phenolic solid residues. The formation of the aromatic char – a highly condensed solid residue – is initiated by the heterogeneous cleavage of the aromatic hydrocarbons such as naphthalene, benzene, and toluene. The phenolic char is formed from the highly reactive phenolic OH groups which accordingly facilitate the formation of the new C–C linkages on the *para*- and *ortho*- positions by forming aldehyde and quinone methide intermediates (Scheme 4) [39,62]. Additionally, condensed structures are formed due to the phenolic OH group interactions with unsaturated side-chain carbons and aromatic rings [62].

Based on the examination of the β -5 and 5–5 model compounds, char

could also be defined as a precursor for the formation of carbon dioxide, water, carbon, and hydrogen if consists of dimers and oligomers linked by either β -5 or 5–5 bond [55]. Char is composed mainly of guaiacyl units [39], accordingly, due to the higher carbon content more solid residue can be expected when the softwood lignin is used [20].

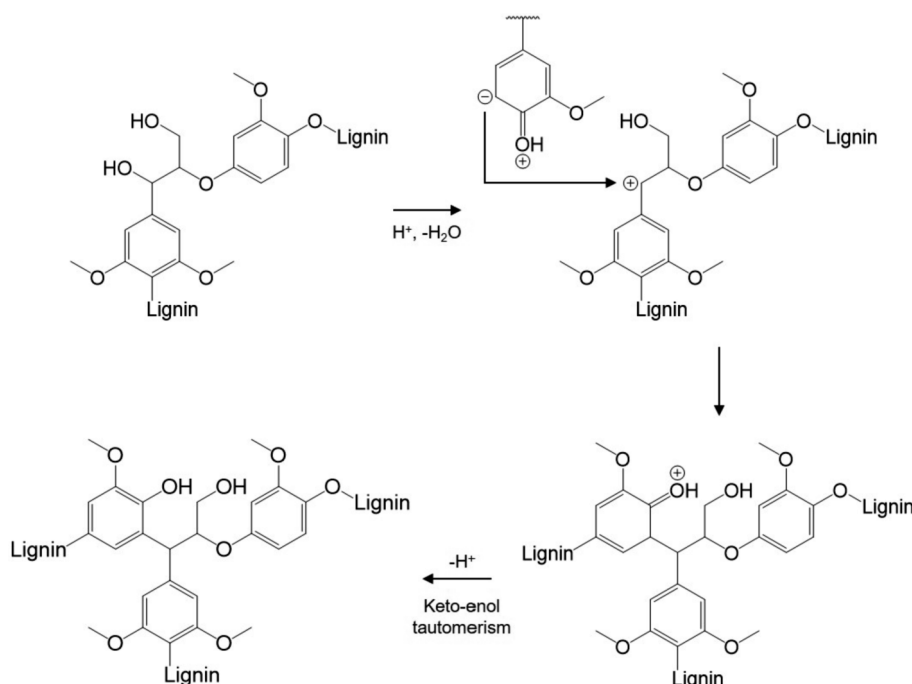
The kinetic modelling study performed by Abad-Fernandez *et al.* [52] proposed that char is formed primarily due to the condensation of the monomeric units during hydrothermal conversion as the reaction rate constant for char creation from monomers was higher than the ones from oligomers and dissolved lignin. However, Forchheim *et al.* [58] indicated the oligomeric units as the main contributors for char formation during catalytic depolymerisation in supercritical ethanol. Obviously, char has an unique formation mechanism that cannot be predicted with high accuracy as it depends on depolymerisation methodology such as initial conditions, reactor system.

A positive effect on the depolymerisation reaction constants was observed while using base or metals (transition, noble) as catalysts, pointing towards more straightforward C–O and C–C bond cleavage. Furthermore, the calculated kinetic constants confirmed the increased *monomers/solid residue* ratio, meaning that the use of base or metal catalysts promoted lignin conversion into monomers consequently forming less solid residue [39,53,58]. As char is formed due to the repolymerisation of the reactive species such as monomers, dimers, larger C–C bond-rich components and since the higher temperatures and longer reaction times are known to favour repolymerisation reactions, the increase of solid fraction with temperature and time is expected [52].

On the other hand, active stabilisation with redox active catalyst or so-called depolymerisation-stabilisation approach applied during RCF of LC biomass, is known to prevent condensation reactions forming minimal amounts of such irreversible solid products [4,63].

3.8. Gas formation

During the LD gases are released. Methane and methanol are formed by removing methyl and methoxy groups from guaiacyl and syringyl units. Both, methyl and methoxy groups, are linked over the weakest bonds, therefore their reactivity increases with temperature [39].



Scheme 4. Proposed reaction mechanism of solid carbon residue formation.

During the depolymerisation at higher temperatures (above 300 °C), CO₂ and CH₄ can be formed from methyl and methoxy substituent groups, while H₂ and H₂O from hydroxyl groups attached to the aromatic ring or to the aliphatic chain. The total amount of CO₂ formed come from both carbonyl and carboxyl functional groups [7]. Some other gases such as CO, H₂S, etc. could be also present. Here, CO is mainly obtained after the water–gas reversal reaction of CO₂, while the gaseous H₂S is reductively generated during heterogeneous catalytic depolymerisation of kraft lignin and lignosulfonates with transition or noble metal catalyst from thiol groups present in the lignin structure [35]. Some C₁–C₃ hydrocarbons could be produced with solvent (methanol, ethanol, etc.) gasification, which is mainly affected by temperature and residence time. Usually, C₂H₆ and C₂H₄, are present in the largest amounts due to the LD in ethanol and its gasification, moreover with a possibility to increase C₂ gas yields at elevated (360–380 °C) temperatures [53].

4. Kinetic modelling of lignin depolymerisation

Recently, kinetic modelling has become an important tool to gain an insight into reaction pathways and link practise to theory, thus mathematically calculating the experimental data and proposing chemical reaction mechanisms [64]. Kinetic modelling plays one of the key roles in scaling-up, describing and understanding catalytic lignin valorisation to predict catalytic behaviour and products, which is not possible with conventional methods. Modelling of the lignin depolymerisation can be defined as an examination at multiple levels, such as multicomponent, multiphase, and multiscale problems usually described in the MATLAB, Python etc. softwares [20]. A general strategy involves comprehension of elementary and secondary reactions, physical steps and transport phenomena.

Lignin is a complex polymer giving a rise to various multicomponent and multiphase products during depolymerisation. The elementary reactions start with lignin depolymerisation into oligomeric products as reaction intermediates. Oligomers can also be converted/depolymerised to smaller fragments such as dimers and monomers. On the other hand, the components in liquid phase can repolymerise forming solid recalcitrant carbon structure (char) and gaseous products from solvent or removed functional groups. The elementary reactions are emphasized within a well-defined lignin structure including the molecular weight distribution, the distribution of monomers and inter-unit linkages as well as an extent of branching [51]. Additionally, the (micro)kinetic model should also take into account the secondary reactions in the solvent, aerosol droplets, and in the gaseous phase [47,49].

In microkinetic models all elementary steps are considered simultaneously and take into account the phenomena at various (multiscale) levels, like reaction kinetics and constants, transport phenomena, and thermodynamics [47,65,66]. As the LD products change phases, the microkinetic models include the dissolution, evaporation, depolymerisation/condensation mechanisms, and the heat transfer during the treatment. In terms of the transport phenomena, the models take into account the thermodynamics at the gas–liquid interface, the mass transfer of gaseous reactant from the gas phase to the liquid, the transport of the liquid component to the surface of the catalyst particles, their adsorption and desorption, and, most importantly, the catalytic rearrangements and degradations on the catalyst surface for all the constituents in the reaction medium [20,47,51]. Kinetic approaches vary depending on the amount of the molecules adsorbed on the catalyst surface and/or active sites, molecular interactions with or without direct adsorption from the gas or liquid phase, or adsorption at adjacent active sites. Models and microkinetic methods usually describe the reaction mechanism occurring on the surface of the catalyst as a rate-limiting step, while other elementary steps are considered significantly faster and are described as being in equilibrium [67].

The development of LD microkinetics is difficult due to the complexity of its structure and several consecutive and parallel

reactions. The microkinetic studies are usually limited by the number of components for which the intrinsic rates can be estimated and the complexity of oligomeric intermediates which structure and corresponding reaction pathway network is often unknown. Although the advanced and expensive characterisation methods (e.g. nuclear magnetic resonance, size exclusion chromatography) are needed to characterised the structure of lignin and its oligomers, the effect of changed structural features (e.g. lignin inter-unit linkages and hydroxyl group content, molecular weight, etc.) has been ignored in recently developed kinetic models for LD. The prospective of extended lumped kinetic models with applied variation of structural features of products could improve the predictive kinetic models to tailor product distribution for implementation of models to accelerate optimization of catalytic technologies and depolymerisation processes. Accordingly, to simplify the global kinetic parameters estimation by reducing reaction complexity and difficulties, the lignin model compounds were introduced to describe microkinetics of lignin moieties. The typical lignin model compounds are monomers or dimers with a particular inter-unit linkage [14,68,69]. Nevertheless, the kinetic studies with the lignin model components are not in the scope of this review and further the emphasis is given on kinetic reaction rates and parameters for the transformation of real lignin samples.

Up till now reported kinetic models describing LD (excluding the pyrolysis), developed explicitly using different types of lignin are summarised in Table 1. Units of the experimental data are unified and recalculated values are accordingly assigned.

Based on the reaction mechanism and kinetic expressions (Scheme 2), a set of differential equations needs to be written (Equations 1–5) to describe LD. The methodology for the simplest lignin kinetics is condensed into a lumped-kinetics approach. LD products are grouped into different lumps according to their similar structure, state of matter or functional groups, e.g., oligomers, monomers, gas and solid phase, etc. [52,53,65]. In the lumped kinetic approach, the lumped model was considered homogeneous and it undergoes the same reaction pathway. For the lumped microkinetic calculations, the first or pseudo-first order modelling is usually related with suitable representation. However, when the lumped model is used, the calculated kinetic parameters include hundreds or thousands individual reactions during the LD.

$$d(\text{lignin})/dt = -(k_1 + k_2 + k_3)(\text{lignin}) \quad (1)$$

$$d(\text{oligomers})/dt = k_1(\text{lignin}) - k_4(\text{oligomers}) \quad (2)$$

$$d(\text{monomers})/dt = k_4(\text{oligomers}) \quad (3)$$

$$d(\text{gas})/dt = k_2(\text{lignin}) \quad (4)$$

$$d(\text{char})/dt = k_3(\text{lignin}) \quad (5)$$

On the other hand, LD pathway with a higher accuracy including well-defined reaction products, their adsorption and desorption rates could be applicable to lignin microkinetics. The molecule-based approach can also be used for microkinetic modelling of LD. The molecule-based model elucidates a complex mechanistic pathway from lignin to the obtained products including various intermediates [9]. The most important advantage of the molecule-based models is the application possibility for different biomass feedstocks for targeted process optimization.

However, the lack of studies with applied chemical reaction kinetics of lignin model components to kinetics of lignin depolymerisation has been observed. There are several studies of lignin monomeric and dimeric model components while the (micro)kinetics of lignin depolymerisation exclude the findings obtained from model component. In our opinion, the combination of (micro)kinetic models is important future aspect and the knowledge from each process is highly expected to be interrelated, similarly as it was done for studies with biomass feedstock and its relevant model component. The organosolv pretreatment process

Table 1
(Micro)-kinetic models of lignin depolymerisation.

Lignin type (wood)	Depolymerisation	Methodology	Experimental						Products (yields, wt %)	Ref.
			Catalyst	Reactor type	Atmo-sphere	Solvent	Flow rate (mL/min); reactor volume (mL); reaction time (min)	Conditions (T, °C; p, MPa)		
Kraft lignin (softwood)	Hydrothermal	Microkinetic model, lumped parameter approach	–	Continuous micro-reactor	n.d.	H ₂ O	26.7–41.7* – 6 × 10 ^{-3*}	370–400 26	LO ^a : 10–40 M: 4.7–10 CH: 5–40 M: 10–20 CH: 70 G: 6–10	[52]
Alkali lignin (softwood)	Hydrothermal	First-order kinetic model	–	PFR	n.d.	H ₂ O	– – 8.3–166.7 × 10 ^{-3*}	390–450 25	M: 10–20 CH: 70 G: 6–10	[39]
Kraft and organosolv lignin ^b (herbaceous)	Hydrothermal	Simplified kinetic model	–	Batch reactor	N ₂	H ₂ O	– 75 10	300–374 22	LO: 75 CH: 20 G: 5	[70]
Alkaline lignin (softwood/hardwood)	Hydrothermal	First-order kinetic model	–	Batch reactor	N ₂	H ₂ O	– 11 5–60	250–350 20	LO: 25–40 CH: 20 G: 10–20	[71]
Enzymatic hydrolysed lignin (softwood)	Hydrothermal	Formal-kinetic lump model	–	Batch reactor	n.d.	H ₂ O	– 5 15–480	320–380 n.d.	M: 3	[58]
Kraft lignin ^c (softwood)	Base-catalysed	Microkinetics model, lumped parameter approach	NaOH	PFR	n.d.	H ₂ O	166.7–333.3 × 10 ^{3*} 1 × 10 ^{6*} 6	240–300 25	O: 85 M: 2.2–3.2	[72]
Protobind 1000 lignin (herbaceous)	Acid-catalysed	Formal-kinetic lump model	Formic acid	Batch reactor, CSTR	n.d.	EtOH	– Batch: 5, CSTR: 190,140	360–400 n.d.	M: 30–40 CH: 2 G: 15	[53]
Lignin (softwood)	RCF	Fitting the extrapolated rate data	Ni/C	Batch reactor, FDBR	H ₂	MeOH	MeOH: 0.5, H ₂ : 50 50 60*	150–215 3	M: 20	[73]
Protobind 1000 lignin (herbaceous)	Hydroconversion	Pseudo-component lumped model	Sulfided CoMoS/Al ₂ O ₃	Semi-batch reactor	H ₂	Tetralin	– 300 0–780*	350 8	O: 8 M: 35	[9]

PFR – plug flow reactor; CSTR – continuous stirred tank reactor; FDBR – flow-through dual bed reactor.

LO – lignin oil; O – oligomer; M – monomers; CH – char; G – gases.

n.d. – no data.

* recalculated value.

^a lignin oil – crude depolymerisation product (low molecular fragments of lignin, monoaromatic products).

^b fast and slow reaction phases.

^c pilot design.

^d mass and transfer limitations included.

supported the findings obtained from the cleavage of benzyl phenyl ether in (aqueous) organic solvents [24,74]. Additionally, Bijok *et al.* [75] considered inherent heterogeneous nature of lignocellulosic biomass in terms of the fundamental chemical component distribution and anisotropic structural properties for modelling the kraft pulping process. The model of the lignin kinetics indicated that the reactivity of lignin during kraft pulping process decreases as the isolation progresses [75,76]. Moreover, Köchermann *et al.* [77,78] applied the kinetics of D-xylose and an aqueous organosolv hemicellulose conversion into furfural, but the improvements of the kinetic model would be required since the activation energies disproved a clear trend of furfural yields between hemicellulose and D-xylose conversion.

4.1. Common assumptions for microkinetic modelling

Understanding of mass and heat transfer, transport phenomena, and molecular interactions is essential for the process systems and microkinetic modelling. For microkinetic model development, the following steps are necessary/required: (i) establishing definitions and assumptions for steady-state or dynamic processes-catalyst particle dimensions, number of active sites; (ii) mass and energy balance development and

their differential equations; (iii) development of algebraic equations to calculate or predict the required properties and variables defined in the differential equations (mass and heat transfer coefficients, diffusivities, heat of desorption, fluid viscosity, density and molecular weight of materials, etc.); setting up the boundary conditions for the reaction system and the environment; and numerical calculations and model simulations or implementations to solve the differential and algebraic equations using the Gear's, the Runge–Kutta or Crank–Nicolson methods [49,51,65].

Kinetic constants and other parameters involved in a chemical reaction are described by a set of differential equations. They are written according to the individually assumed reaction mechanism, usually taking into account the following assumptions: organic and gas (hydrogen) molecules adsorb on the catalyst metal surface where the reaction can occur, although organic compounds could theoretically adsorb on the support surface and thus could not react with hydrogen; all the available adsorption sites are independent and equivalent; and only one organic molecule or hydrogen atom can adsorb on an active site [47,52]. Different assumptions could be made using lignin model compounds. Since the reactant and products have similar structures, the adsorption and desorption constants could be considered equivalent

[8,79]. A few assumptions could be made regarding the reactor system and process, for instance that the system followed the ideal reactor design with a homogeneous mixing and density through the process [53]. Additionally, it is usually assumed that all the reactions during LD occurs in the liquid phase [9].

After specified assumptions, written differential equations, and quantitative sample analysis, the obtained experimental data is modelled by fitting it to a set of differential equations [52,71]. The fitting is done by minimizing the absolute error between the calculated and experimental yields [52]. However, the reaction rate constants predicted by different mathematical models, approaches, and fits can vary by about 2 to 4 orders of magnitude for similar reaction types [8,58]. Nevertheless, the high error in the kinetic parameters may indicate that the assumption and model do not follow (pseudo)-first order reaction kinetics with great accuracy [71].

4.2. Kinetic constants in supercritical water

In recent years, researchers have focused on the use of more sustainable solvents such as water. Water under subcritical and supercritical conditions exhibits a wide range of physical and chemical properties, which makes it attractive to be used as a solvent in lignin chemistry [39].

The activation energy of the primary LD in solvent can vary depending on lignin structure with respect to the plant source and the methodology used to isolate lignin from biomass [39,70]. The LD constants studied followed an Arrhenius equation. The authors used similar reaction conditions but different reactor systems (batch or flow-through reactors), therefore some variations in activation energies were observed [53,73]. Further discussion follows in the *Transport Phenomena* section.

The literature review about the kinetic parameters in supercritical water showed that many parameters principally affect LD [58]. For the purpose of this work and for clarity we summarized kinetic parameters in Fig. 5. Data is presented in Arrhenius plot which allows visualizing and simply calculating the activation energies. The average activation energy of overall LD was $34.5 \pm 1.5 \text{ kJ mol}^{-1}$ [39,58,70], while the one from the reaction rates reported by Obeid *et al.* [71] and Abad-Fernandez *et al.* [52] deviated significantly 45.9 kJ mol^{-1} and $222.5 \text{ kJ mol}^{-1}$, respectively. Otherwise, kinetics of the base-catalysed LD studied by Bernhardt *et al.* [72] showed lower activation energies in

aqueous solution of 1.67 and 2.50 wt% sodium hydroxide with corresponding energies of 37.1 and 21.6 kJ mol^{-1} , respectively. The high variability of the kinetic parameters in the supercritical water could be affected by the specific water properties under reaction condition-dependent water properties.

The main reason for the deviations from some authors can be explained by various reaction conditions (pressure, heating rate, etc.), definition of the depolymerisation route, solubility and decomposition of lignin, intramolecular interactions, solvent, depolymerised low-molecular weight fragments, and most importantly: the type of lignin [53,58,71].

4.3. Demethylation and demethoxylation in supercritical solvents

Demethylation is attained by the cleavage of the aryl–O–methyl ether bond. Since the aromatic ring and hydroxyl groups are more stable [58], the bond containing methyl functional group is predominantly cleaved during the depolymerisation process. The prompt cleavage of the aryl–O–methyl ether bonds was confirmed by Pu *et al.* [9], as a rapid conversion of methoxyphenols to catechols and alkylphenols. Studies with methyl-substituted phenolic moieties suggested that the reactivity of the methyl-substituted groups is strongly affected due to the steric hindrance, however later it was shown that the intrinsic differences in electronic structure control the reaction rates rather than geometric effects [79].

Interestingly, demethylation of the methoxyphenols in lignin structure showed comparable activation energies, regardless of the lignin type and the solvent used for the selected process conditions [58]. However, differences were observed between the rate constants depending on continuous stirred tank reactor (CSTR) or batch reactor was used for the treatment (Table 2). Overall, the LD to methoxyphenols indicates up to 1000-times higher rate constants in CSTR than in batch reactor, the only exception is demethylation to catechols which progressed with similar reaction rates [53]. In addition, variations between the reaction rate constants of methoxyphenols conversion to phenols were observed using lignin model compounds (isoeugenol, guaiacol, etc.) [60,80,81]. Therefore, the kinetic parameters cannot be compared empirically because of the different reaction conditions, catalysts used, and the different structure of the reactants.

4.4. Kinetic constants of metal-catalysed lignin depolymerisation

Metal catalysts have been used for several lignin hydrotreatment processes to maximize yields, selectivity, and to lower the energy barrier of conversion into the desired components. Activation energies of the LD using Ni/C as a catalyst were measured and compared in batch and flow-through dual bed reactor (FDBR) by Anderson *et al.* [73]. The activation energy of LD in the batch reactor with the larger catalyst particles (500–1000 μm) was 33 kJ mol^{-1} , while it increased to 39 kJ mol^{-1} when the size of the catalyst particles was reduced (75–250 μm). The opposite was observed during LD in FDBR. Here, the activation energy was 58 kJ mol^{-1} using large catalyst particles, which decreased to 53 kJ mol^{-1} with smaller pellet size. Thus, the highest activation energy of LD with metal catalysts obtained is 58 kJ mol^{-1} [9,73], while studies with lignin model components showed higher activation energy for the reduction and cleavage of the aryl ether bond already at the beginning of the process, although the higher monomer yields were obtained from dimeric structures compared to the real biomass. The activation energy values varied depending on the dimer model component, conditions, and catalyst type used, ranging from 85 kJ mol^{-1} for diphenyl ether [14,82] to 170 kJ mol^{-1} for 1-(3,4-dimethoxyphenyl)-2-(2-methoxyphenoxy)propane-1,3-diol [73].

The activation energies for the depolymerisation of lignin to the target monomers are extraordinarily different depending on the reaction conditions. For instance, in the particular supercritical solvents the activation barrier is lower compared to the metal-catalysed system

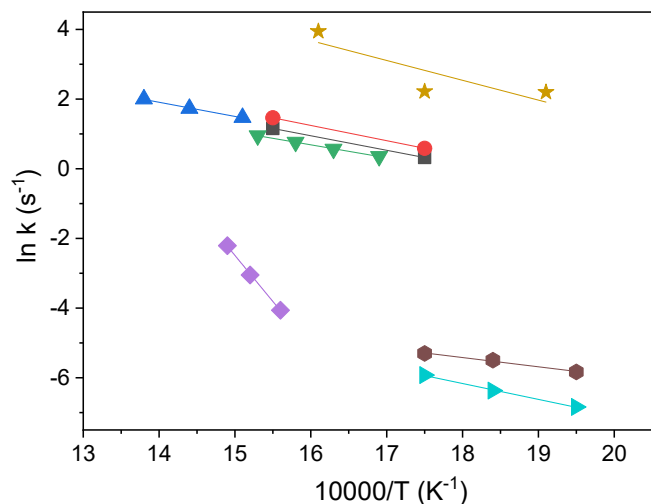
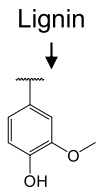
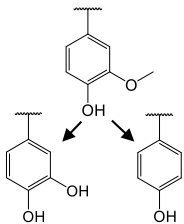
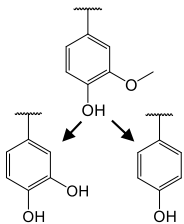
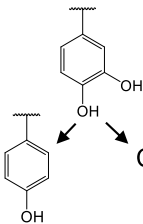
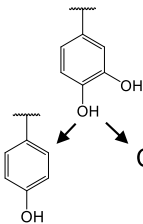
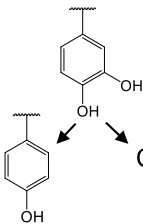


Fig. 5. Arrhenius plot for lignin overall depolymerisation; kinetic parameters reported by: (7) Yong *et al.* 2012 [39], (B) Forchheim *et al.* 2014 [58], (!) Zhang *et al.* 2008 [70], (β) Bernhardt *et al.* 2021 (1.67 wt% NaOH) [72], (μ) Bernhardt *et al.* 2021 (2.50 wt% NaOH) [72], (Δ) Abad-Fernandez *et al.* 2020 [52], (ξ) Obeid *et al.* 2020 [71].

Table 2
Kinetic parameters for demethylation reaction calculated for 360 °C (k_1), and 380 °C (k_2) [53,58].

Reactor system	Solvent	Reaction type					
							
CSTR	EtOH	k_1 (s ⁻¹)	4.9×10^1	3.1×10^{-1}	n.d.	6.8×10^{-2}	1.4×10^0
		k_2 (s ⁻¹)	7.2×10^1	5.9×10^{-1}	n.d.	1.2×10^{-1}	2.1×10^{-1}
		E_a (kJ mol ⁻¹)	6.8×10^1	1.1×10^2	n.d.	9.2×10^1	9.0×10^1
Batch reactor	EtOH	k_1 (s ⁻¹)	4.8×10^{-2}	5.2×10^{-1}	n.d.	1.3×10^{-4}	6.5×10^{-1}
		k_2 (s ⁻¹)	n.d.	n.d.	n.d.	n.d.	n.d.
	H ₂ O	k_1 (s ⁻¹)	2.4×10^{-2}	5.8×10^{-1}	1.0×10^{-1}	1.6×10^{-2}	$< 6.0 \times 10^{-5}$
		k_2 (s ⁻¹)	3.4×10^{-2}	1.1×10^0	1.8×10^{-1}	2.3×10^{-2}	$< 6.0 \times 10^{-5}$
		E_a (kJ mol ⁻¹)	5.8×10^1	1.0×10^2	9.4×10^1	5.5×10^1	3.0×10^3

n.d. – not determined.

[39,58,73], highlighting the importance of screening the most suitable set-up.

4.5. *Ab initio* lignin microkinetics

The aim of the microkinetic model development is to understand lignin behaviour under the mild hydroprocessing conditions. It has to be considered that the kinetic model, developed based on the lab-scale experimental data, does not guarantee the integration of the same modelling approach for a higher scale. As the lumped kinetic models and the global kinetic parameters have been proposed, the disadvantages connected to the insufficient data about the depolymerisation mechanisms represent a major challenge for introducing the microkinetics for each LD step. Furthermore, high variety of the reaction products, different interconnectivity of the building blocks and a large number of the reactions, occurring during the hydrotreatment represent another challenge to be solved. Effective modelling requires comprehensive data about the lignin structure as well as the structure of the oligomeric fragments, thus at the end increasing the model complexity with each reaction intermediate and product included.

Determination of the microkinetics for LD, proposes an opportunity to generate automated mechanism discerning reaction pathway, similarly as emphasized in the review of lignin pyrolysis microkinetics [51]. The automated mechanism design approach will finalise the reaction pathway by consecutive application of the reactions involving all the reaction products. The smaller molecules (e.g. lignin model compounds) are more accessible for the reactive catalyst, solvent or atmosphere, while the reaction mechanism involving larger molecules (e.g. lignin oligomeric components, lignin) is more complex. At some point lignin depolymerisation products may be identical to the lignin model compounds, therefore it justifies the implementation of the kinetic data from small to larger molecules. In addition, lignin depolymerises into the smaller constituents with the known kinetic data [83] revealing the importance of the lignin model components to the overall lignin depolymerisation microkinetics.

For the LD microkinetic study the better understanding of the typical lignin bond cleavage in model compounds could be attained using an *ab initio* computational methods. *Ab initio* screening approach with density functional theory (DFT) and molecular dynamic was developed for the identification of the potential depolymerisation mechanisms for lignin oligomers composed of 2 to 6 phenolic rings. It was proposed that the cleaved bonds can destabilize adjacent bonds, causing successive cleavage [84].

In the way of deeper understanding of LD microkinetic models, the *ab initio* methods with lignin model compounds enrich the research field of lignin providing a key fundamental data to facilitate the development of models. Lignin valorisation is about maximizing the selectivity of lignin conversion into monoaromatics and reducing the solid residue, thus it is of importance to solve the challenge of the microkinetic modelling turning it into the tool enhancing LD efficiency.

5. Transport phenomena

Products obtained during the lignin depolymerisation and eventual hydrogen reactant transfer through phases (of states) which should be considered in a multiscale model to distinguish between the intrinsic and overall kinetic rate in for the given reaction, and to evaluate the contribution of mass and heat transfer resistance. The reaction mechanisms and kinetic rate expressions are the fundamentals for the optimisation of the LD process. Mostly the lumped kinetic models have been proposed with competitive and/or simultaneous multi-stage reactions to global products schemes [85], however with the insufficient consideration given to mass and heat transfer [76,86]. Transport phenomena and phase transitions (solid polyaromatic fractions can melt at reaction temperature) involve gas dissolution in the liquid phase, a transfer through the gas bubbles, liquid films, catalyst particles (in packed-bed) and its pores (in stirred and packed-bed operation), adsorption and desorption of the molecules, and chemical transformations of the adsorbed components (Fig. 6) [8]. The review of the mass transfer overviews the transport phenomena of compounds through liquid or gaseous phase within the catalyst or lignin (biomass feedstock) particles, while phase transition subsection is focused on lignin dissolution and gas solubility in the reaction media (lignin-solvent liquor).

5.1. Mass transfer

It has been already reported that the LD kinetic rates are affected by the structure of the examined lignin and the solvent nature. Understanding of the depolymerisation limitations caused by the lignin structure and solvent is important for screening different catalysts and investigating a suitable reactor system. A coupled reaction–diffusion model can be used to predict the transport limitation in specific reaction media and systems. In heterogeneous catalysis, the rate of mass transfer of lignin and intermediate(s) from the liquid phase to the solid surface can significantly influence intrinsic reaction rates, even selectivity and reaction mechanism [88]. Theoretically, the intrinsic (maximum)

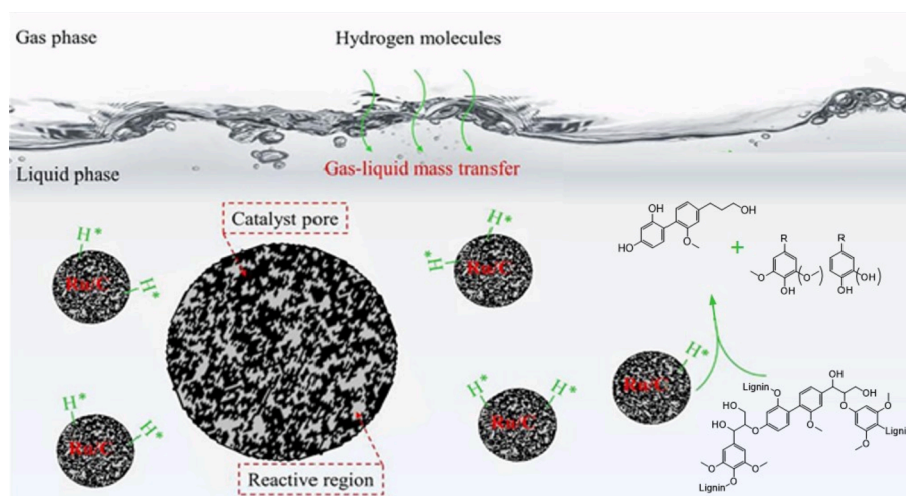


Fig. 6. A schematic representation of gas phase transfer at the gas–liquid interface, gas solubility and diffusion, chemical reaction at reactive sites and diffusion of component (intermediate) in catalyst pore and bulk phase. Adapted with permission from Wei *et al.* [87].

kinetic rates of LD are achieved when mass transport is eliminated and the concentration of components in the catalyst pore is zero [73]. Therefore, to avoid mass transport limitations highly diluted systems, low active sites loading and smaller catalyst particles are advised to be chosen [53].

For the determination of the realistic activation barrier for lignin, eliminating the effects of the depolymerisation reactions, the mass transport limited batch reactor was replaced by the kinetically-limited FDBR [73]. The variance between the yields of the recovered components (monomers, char, gases) and the kinetic parameters was found in both, batch and flow-through reactor systems (FDBR, CSTR, PFR) [9,53,73]. Generally, the amount of the gaseous phase and solid carbon residue yields were 2-times higher in batch reactor than in CSTR, as it operates at lower (outlet) concentration of reactive lignin species. Additionally, gas composition was affected by the reactor type as well. Monomer yields were found to be dependent more on reaction conditions compared to gaseous and solid components, specifically, 15–30 % lower monomer yields were attained in batch reactor than in CSTR [53].

Lignin depolymerisation examination in ethanol using the CSTR and batch reactor, identified CSTR to be more efficient in terms of rate coefficients [53]. The calculated kinetic constants of the elementary depolymerisation for the CSTR system were much higher compared to the batch reactor, indicating a higher yields of the phenolic monomers, lower amounts of recovered solids and gas products. The rate constant values for the formation of monomers (*e.g.* methoxyphenols, (ethyl) phenols) in the CSTR were 1000-times higher compared to the batch reactor, together with only minor effects on gasification and formation of the solid residue. These findings confirm the selection of the reactor system to play a key role on the quantity of the produced gaseous components as well as the solid carbon residue.

A complex study on LD using a FDBR and batch reactor loaded with different sizes of catalyst particle (75–250, 500–1000 μm) was carried out by Anderson *et al.* [73]. Activation energies for small and large catalyst particles were similar, which confirmed the absence of the limitations due to the mass transfer in the FDBR, while using the batch reactor activation energies increased with a smaller catalyst particle. Therefore, it draws a conclusion that the reaction rate of LD in batch system was limited by the internal mass transfer, which accordingly decreased with a reduced particle size. Moreover, the mass transfer phenomena in batch reactor is affected by many parameters, including lignin particle size, catalyst particle size, active site density, porosity, stirring rate, stirrer design and reactor geometry which impact process performance.

Kinetic parameters and mass transfer resistances for lignin and its

model components were also examined in microreactors. Microreactors can be used to predict which phenomena and factors affect the mass and heat transfer rates, which is essential for determination of the global kinetic parameters.

The limitations of the internal mass transfer depend on the concentration gradient within the catalyst particle and could be roughly estimated by calculating the Thiele modulus and the effectiveness factor. If the Thiele modulus is below 0.5, the effectiveness factor is close to 1, indicating that the reaction is kinetically limited, which means that the reaction occurs under the same conditions within the catalyst pellet and at the particle surface [10,60].

To evaluate the limitations of the pore diffusion, the size of the catalyst particles can be varied. The increased particle size altered intraparticle transport and diffusion within the pore, affecting the concentration profile within the catalyst pellet [10,60,73]. The reaction is diffusion limited within the particle as the value of the Thiele modulus increases, and the effectiveness factor decreases with the larger particles. Diffusion limitation within the particle is the main reason for the reduced reactant conversion, additionally confirmed by the modelling results of Hafeez *et al.* [10]. The reported kinetic model evaluates the overall reaction rate, which can be enhanced by reducing the catalyst particle size, increasing the inner surface area, temperature, and the concentration of reactant [10,60]. In kinetic regime where very fine particles were used, mass transfer limitation also appeared after the catalyst was deactivated *in situ* by side products formed on the catalyst surface [88,89], especially solid residue formed during LD. This effect should not be confused by chemical catalyst poisoning (not forming a physical barrier) which can alter intrinsic kinetic behaviour and surface rates [90]. Therefore, a multiscale model should consider actual mechanisms that cause apparent decrease of activity to be appropriately attributed to either mass transport limitation or altered activity of the active surface.

An example of good practice involved the contributions of intrinsic kinetics, intraparticle and interparticle diffusion and transport phenomena in bulk phase(s) on various scales over silica (SBA-16)-supported catalyst, however only for the simplified system of ethanol to butadiene conversion (Fig. 7) [91]. The external mass transfer limitations include the mass transfer examination through the gas–liquid and further the liquid–solid diffusion at the interface of the catalyst particle. The elimination of the external mass transfer can be accomplished by maximizing the flow velocity, resulting in a thin boundary layer, and the concentration in reaction mixture (bulk concentration) is approximately equal to the concentration on the surface of the catalyst particle [10,60]. Even though the internal and external mass transfer studies were

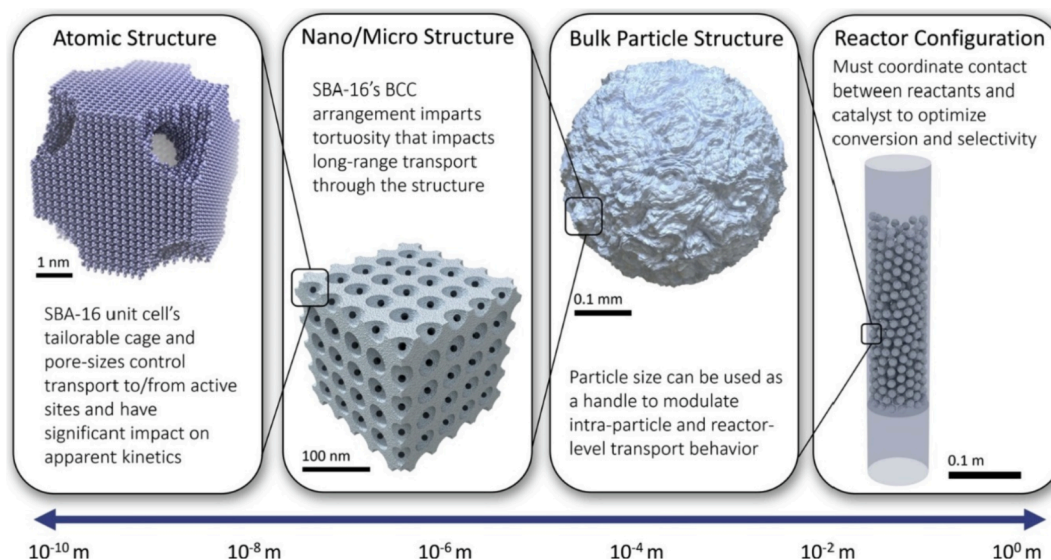


Fig. 7. Representative multiscale model for transport phenomena with contributions of intrinsic kinetics, intraparticle diffusion, interparticle diffusion and bulk transport. Reprinted with permission from Bharadwaj *et al.* [91].

performed in the microreactor, the guidelines are helpful for understanding the transport phenomena in the conventional batch/flow-through (FDBR, CSTR, PFR) reactors. Consequently, the determination and optimisation of the LD rates it is of importance as well as error elimination for the most commonly used reactors (batch, CSTR, PFR).

On the other hand, tandem transport phenomena on mesoscale (intermediate regime between the molecular and reactor scale) for biomass conversion and catalytic processes has been reviewed by Ciesielski *et al.* [90] as process optimization for lignin (biomass) valorisation to fill the gap between research and bioenergy for lignocellulosic feedstock. Mass transfer limitations of biomass pretreatment methods and/or biomass pyrolysis have been more extensively investigated compared to mass transfer limitations of catalytic lignin depolymerisation under mild reaction conditions. Nevertheless, the trends and knowledge obtained from these studies could be informative with highlighted barriers for future lignin valorisation as biomass feedstock introduces significant transport limitations. Thornburg *et al.* [92,93] and Luterbacher *et al.* [94] studied transport phenomena and pore-hindered diffusion to predict the biomass fractionation with rate-limiting steps. The critical biomass particle size to eliminate intraparticle diffusion has been 0.2 mm for lignin-first biomass fractionation [92] and 0.05 mm for enzymatic hydrolysis of biomass [94] while unsorted corn stover deacetylation has been mass transfer-limited process for particles larger than 2.3 mm in length [93]. Relationship between effectiveness factor and Thiele modulus has been previously described for catalyst particles [10], however, kinetically- and/or diffusion-limited regimes for biomass particle size have been found with similar relationship [92,93]. Thus to relate real biomass feedstock studies to lignin samples and kinetically-limited behaviour for depolymerisation small lignin particle size should be used.

5.2. Heat transfer

Lignin is a deficient heat conductor mainly due to the amorphous orientation of monolignols in the macromolecule. Low thermal conductivity promotes substantial temperature gradients within particles which are additionally influenced by their shape and size [86,95]. Similarly to mass transfer, the heat transfer can be described in various controlled regimes: non-controlled conditions, external heat transfer controlled, kinetics controlled and internal heat transfer controlled. The analogy between the mass and heat transfer limitations can be analysed based on their two constitutive equations: Fick's law of diffusion and

Fourier's law of heat conduction. Generally, heat transfer limitations are less significant in solvent reaction media, because liquids tend to have high heat capacity and thermal conductivity relative to gases [88].

However, the heat transfer limitations have been mainly introduced for biomass pyrolytic conditions where heat phenomena and heating rate have been a critical factors for the effective rate of pyrolysis (pyrolysis rate of single particle) for desirable product yields [96–98]. The particle heating rates and temperature gradients have been assessed by solving mathematical models with assumptions regarding the biomass geometry with the spherical particle shape. Though Ciesielski *et al.* [99] illustrated that the spherical particle shape departs from accurately captured intraparticle temperature gradient. Also the assumption of isothermal biomass particle (negligible intraparticle transport) has limitations as it is valid only for very small particle size (e.g. the range of 100–1000 μm in a fluidized bed reactor), thus biomass particle should be assumed nonisothermal [100]. Furthermore, the differences between the biomass particle and pore structure of pine and poplar wood corresponded in different external heat coefficients [101]. For further reading on dominant transport phenomena of biomass pyrolysis systems, Brennan Pecha *et al.* [86] and Ciesielski *et al.* [90] research groups recently published extensive review articles.

The intraparticle heat transfer has been ignored in studies of (micro) kinetic models for lignin depolymerisation. Nevertheless, it has minor effect as the lignin is dissolved beforehand reaching the final reaction conditions. Convective heat transfer between a reactor surface and a moving solvent has major influence under the supercritical conditions and it is reasonable to consider the solvent properties which vary with the temperature, especially near the pseudo-critical line [102,103]. On the other hand, inhomogeneity of solvent and discontinuous property changes are unlikely to have significant influence on heat transfer phenomena above the critical temperature, *i.e.* phase transition.

5.3. Phase transition

The phase transition phenomena is more critical for the optimisation of the catalytic LD, similarly as the mass transfer to the catalyst particles. It is a multilevel phenomenon as three phases (solid – lignin, liquid – solvent, gaseous atmosphere) are included in LD process.

The understanding at solid–liquid interface is currently much more developed in comparison to the knowledge of the molecular details at liquid–gas interface or gas solubility parameters in lignin dissolved reaction media. The solubility of lignin in solvent (solid–liquid interface)

needs to be described with the appropriate solubility parameter – solubility factor (δ -value). The organic solvent–water media were used for organosolv isolation process to consider lignin solubility and it was proven that the highest solubility is achieved in 75 vol% organic solvents (ethanol, acetone, tetrahydrofuran, dioxane). Additionally, it was observed that the delignification increased with the process temperature up to 210 °C [104] while the differences of isolated lignin structural features have not been discussed. The maximum solubility of lignin is reached in solvents with similar δ -value as the lignin has, for example 75 vol% ethanol/water media (δ -value: 31.7 MPa^{1/2}). The Hildebrand solubility parameter of lignin generally ranges of 24.5–31.7 MPa^{1/2} while the real δ -value of a polymer has been estimated based on the contributions of atomic and functional groups with the known structure of the repeating unit (e.g. phenylpropane units in lignin). Therefore, δ -value depends on the ratio of the G-, S- and H-units present in lignin [105]. The study by Ni and Hu [106] reported maximum solubility of the lignin in 70 vol% ethanol solution which is comparable to the study carried out by Goldmann *et al.* [107] and Ye *et al.* [105] with stated highest solubility in 60 vol% and 65–75 vol% ethanol/water solution, respectively. Similarly, the highest lignin solubility has been reached in 75 vol% acetone, 75 vol% dioxane and 75 vol% tetrahydrofuran with the values of solubility parameter at 29.5, 28.7 and 28.0 MPa^{1/2}, respectively [104,105]. On the other hand, 75 vol% methanol/water solution was found to be less efficient solvent for lignin with the value of the Hildebrand solubility parameter at 33.9 MPa^{1/2} [24]. In summary, lignin has the highest solubility in 75 vol% solutions of aforementioned organic solvents while it is not trivial that lignin isolated from different biomass source would attain the same dissolution.

Recently, Soares *et al.* [108] and Sosa *et al.* [109] investigated lignin solubility in (aqueous solutions) of several deep eutectic solvents (DES). The efficiency of lignin dissolution in DES based on cholinium chloride has been governed by chemical nature (carboxylic or alcohol) of DES hydrogen bond donors, chain length and molar ratio to hydrogen bond acceptors while the addition of water negatively affected lignin solubility in DES [109]. Additionally, the isolation process (kraft, organosolv, etc.) from the same type of wood influenced lignin solubility [108].

The increase of the solvent hydrogen bond capacity accordingly improves lignin solubility [106] which accordingly facilitates the change of phases within the catalytic reaction. Here, dissolved lignin macromolecules and liquid intermediates change phases several times forming gaseous, liquid and solid residual components. Inside liquid reaction mixture (phase), gaseous products are formed by chemical defunctionalisation reaction, while solid residue formed by condensation may be adsorbed on heterogeneous catalyst which lower its catalytic activity. The existence of phase changes within the reaction mixture critically affects attempts to define mass transfer during LD [86]. At the end, all of those phase changes are kinetically described by kinetic rates for each individual step.

Gas solubility is another important aspect to be explored [110,111] as hydrogen is mainly used as a H-donor to provide and form the reactive OH radicals which are involved in almost every reaction during LD. Therefore, the solubility of hydrogen is of the utmost importance for LD modelling. Despite the numerous solubility studies performed in conventional organic solvents [112–114], there is the lack of the hydrogen solubility data in lignin-derived liquids, as it was explored, for instance, in furfural and furfuryl alcohol with the aim to design the accurate kinetic model describing defunctionalisation processes [110]. Wei *et al.* [87] hydrogenated levulinic acid and developed multiphase transport model to simulate its conversion while modified pseudopotential model was applied for gas–liquid interface. The levulinic acid consumption rate was found to be determined by dissolved hydrogen and temperature above critical concentration value. As expected, the partial pressure of hydrogen (or any other gaseous atmosphere) could have a great influence on reaction and reaction rate, but can also be a limiting factor due to the coverage occupying active sites on the catalyst.

6. Conclusion and future aspects

The review describes lignin depolymerisation aspects where mechanisms, chemical reaction kinetics and transport phenomena have been presented. Through the literature review, it was observed that in lignin research the main focus has been on the selective cleavage of C–O and C–C bonds with reasonable yields and minor condensation to recalcitrant products rather than on the process optimisation. Non-catalytic and catalytic processes of LD form products with different structural features, yet some has still been structurally unspecified (e.g. lignin oligomeric components, solid carbon residue). The structure of lignin oligomers and carbon residue are less explored therefore, the future investigation of lignin depolymerisation mechanism should include detailed characterisation of lignin lighter fractions and oligomeric components to define its structure. Considering this, the mechanism would be more comprehensive which will improve the development of the kinetic models and consequently the fitting of the kinetic parameters for each defined step within lignin depolymerisation.

Kinetic models reported in the literature are not able to describe an overall depolymerisation process as it is mainly focused on studies with lignin monomeric and dimeric model compounds. The complex lignin structure and a high variety of depolymerisation products have encouraged researchers to group products into kinetic lumps in order to obtain reasonable values for kinetic parameters (summarized in Tables 1 and 2). However, the limitations have still been observed as high differences between activation energies for overall lignin depolymerisation have been reported.

Future studies on chemical reaction kinetics should involve the comprehensively defined lignin fractions or model compounds with 3 to 5 phenolic rings as intermediary stage to lignin macromolecule which would consequently disclose reaction specifics considering the catalytic activity, process mechanism and optimization. As a result, lump kinetic model could be remarkably improved by replacing lumps with a detailed reaction pathway allowing more efficiently to describe catalytic lignin depolymerisation more efficiently compared to the model developed using lignin model compounds.

The lignin depolymerisation has shown multiscale problems for predictive modelling where the transport phenomena is another key parameter to be explored to define the suitable reactor systems. Flow-through reactors (FDBR, CSTR, PFR) were identified as the most efficient set-up for depolymerisation verified with the kinetic model as less diffusion limited process. Since most of the experiments reported are batch processes, it is reasonable to consider using the flow-through reactors processing in future work.

Computational chemistry and modelling calculations have offered a possibility to predict the reaction course based on a reduced amount of the experiments. Even though the development of lignin kinetic models is in progress, the increasing accuracy of the methods and the development of the more complex controllable systems describing lignin depolymerisation using multiscale modelling will certainly improve lignin valorisation.

Declaration of Competing Interest

The authors declare that they have no known competing financial interests or personal relationships that could have appeared to influence the work reported in this paper.

Acknowledgements

This work was supported by the Slovenian Research Agency (research core funding P2–0152 and research project J2–2492).

References

- [1] S.S. Wong, R. Shu, J. Zhang, H. Liu, N. Yan, Downstream processing of lignin derived feedstock into end products, *Chem. Soc. Rev.* 49 (2020) 5510–5560, <https://doi.org/10.1039/d0cs00134a>.
- [2] X. Liu, F.P. Bouxin, J. Fan, V.L. Budarin, C. Hu, J.H. Clark, Recent advances in the catalytic depolymerization of lignin towards phenolic chemicals: a review, *ChemSusChem* 13 (2020) 4296–4317, <https://doi.org/10.1002/cssc.202001213>.
- [3] J.Y. Kim, J. Park, U.J. Kim, J.W. Choi, Conversion of lignin to phenol-rich oil fraction under supercritical alcohols in the presence of metal catalysts, *Energy Fuels* 29 (2015) 5154–5163, <https://doi.org/10.1021/acs.energyfuels.5b01055>.
- [4] T. Renders, S. Van Den Bosch, S.F. Koelewijn, W. Schutyser, B.F. Sels, Lignin-first biomass fractionation: the advent of active stabilisation strategies, *Energy Environ. Sci.* 10 (2017) 1551–1557, <https://doi.org/10.1039/c7ee01298e>.
- [5] W. Schutyser, T. Renders, S. Van Den Bosch, S.F. Koelewijn, G.T. Beckham, B. F. Sels, Chemicals from lignin: an interplay of lignocellulose fractionation, depolymerisation, and upgrading, *Chem. Soc. Rev.* 47 (2018) 852–908, <https://doi.org/10.1039/c7cs00566k>.
- [6] Z. Sun, B. Fridrich, A. De Santi, S. Elangovan, K. Barta, Bright side of lignin depolymerization: toward new platform chemicals, *Chem. Rev.* 118 (2018) 614–678, <https://doi.org/10.1021/acs.chemrev.7b00588>.
- [7] D.F. Payne, P.J. Ortoleva, A model for lignin alteration - part I: a kinetic reaction-network model, *Org. Geochem.* 32 (2001) 1073–1085, [https://doi.org/10.1016/S0146-6380\(01\)00080-8](https://doi.org/10.1016/S0146-6380(01)00080-8).
- [8] A. Bjelić, M. Grilc, B. Likozar, Catalytic hydrogenation and hydrodeoxygenation of lignin-derived model compound eugenol over Ru/C: Intrinsic microkinetics and transport phenomena, *Chem. Eng. J.* 333 (2018) 240–259, <https://doi.org/10.1016/j.cej.2017.09.135>.
- [9] J. Pu, D. Laurenti, C. Geantet, M. Tayakout-Fayolle, I. Pitault, Kinetic modeling of lignin catalytic hydroconversion in a semi-batch reactor, *Chem. Eng. J.* 386 (2020), 122067, <https://doi.org/10.1016/j.cej.2019.122067>.
- [10] S. Hafeez, E. Aristodemou, G. Manos, S.M. Al-Salem, A. Constantinou, Computational fluid dynamics (CFD) and reaction modelling study of bio-oil catalytic hydrodeoxygenation in microreactors, *React. Chem. Eng.* 5 (2020) 1083–1092, <https://doi.org/10.1039/d0re00102c>.
- [11] M.V. Galkin, J.S.M. Samec, Lignin valorization through catalytic lignocellulose fractionation: a fundamental platform for the future biorefinery, *ChemSusChem* 9 (2016) 1544–1558, <https://doi.org/10.1002/cssc.201600237>.
- [12] S. Gillet, M. Aguedo, L. Petitjean, A.R.C. Morais, A.M. Da Costa Lopes, R. M. Lukasiak, P.T. Anastas, Lignin transformations for high value applications: Towards targeted modifications using green chemistry, *Green Chem.* 19 (2017) 4200–4233, <https://doi.org/10.1039/c7gc01479a>.
- [13] S. Bertella, J.S. Luterbacher, Lignin Functionalization for the production of novel materials, *Trends Chem.* 2 (2020) 440–453, <https://doi.org/10.1016/j.trechm.2020.03.001>.
- [14] A. Bjelić, B. Likozar, M. Grilc, Scaling of lignin monomer hydrogenation, hydrodeoxygenation and hydrocracking reaction micro-kinetics over solid metal/acid catalysts to aromatic oligomers, *Chem. Eng. J.* 399 (2020), 125712, <https://doi.org/10.1016/j.cej.2020.125712>.
- [15] A. McVeigh, F.P. Bouxin, M.C. Jarvis, S.D. Jackson, Catalytic depolymerisation of isolated lignin to fine chemicals: Part 2-process optimisation, *Catal. Sci. Technol.* 6 (2016) 4142–4150, <https://doi.org/10.1039/c5cy01896j>.
- [16] W. Jin, L. Pastor-Pérez, D.K. Shen, A. Sepúlveda-Escribano, S. Gu, T. Ramirez Reina, Catalytic upgrading of biomass model compounds: novel approaches and lessons learnt from traditional hydrodeoxygenation – a review, *ChemCatChem* 11 (2019) 924–960, <https://doi.org/10.1002/cctc.201801722>.
- [17] C. Xu, R.A.D. Arancon, J. Labidi, R. Luque, Lignin depolymerisation strategies: towards valuable chemicals and fuels, *Chem. Soc. Rev.* 43 (2014) 7485–7500, <https://doi.org/10.1039/c4cs00235k>.
- [18] A.J. Yanez, W. Li, R. Mabon, L.J. Broadbelt, A stochastic method to generate libraries of structural representations of lignin, *Energy Fuels* 30 (2016) 5835–5845, <https://doi.org/10.1021/acs.energyfuels.6b00966>.
- [19] Z. Zhang, D.S. Zijlstra, C.W. Lahive, P.J. Deuss, Combined lignin defunctionalisation and synthesis gas formation by acceptorless dehydrogenative decarbonylation, *Green Chem.* 22 (2020) 3791–3801, <https://doi.org/10.1039/d0gc01209b>.
- [20] E. Ranzi, P.E.A. Debiagi, A. Frassoldati, Mathematical modeling of fast biomass pyrolysis and bio-oil formation. Note I: kinetic mechanism of biomass pyrolysis, *ACS Sustain. Chem. Eng.* 5 (2017) 2867–2881, <https://doi.org/10.1021/acsschemeng.6b03096>.
- [21] Y. Li, B. Demir, L.M. Vázquez Ramos, M. Chen, J.A. Dumesic, J. Ralph, Kinetic and mechanistic insights into hydrogenolysis of lignin to monomers in a continuous flow reactor, *Green Chem.* 21 (2019) 3561–3572, <https://doi.org/10.1039/c9gc00986h>.
- [22] A. Anca-Couce, I. Obernberger, Application of a detailed biomass pyrolysis kinetic scheme to hardwood and softwood torrefaction, *Fuel* 167 (2016) 158–167, <https://doi.org/10.1016/j.fuel.2015.11.062>.
- [23] T.I. Korányi, B. Fridrich, A. Pineda, K. Barta, Development of ‘lignin-first’ approaches for the valorization of lignocellulosic biomass, *Molecules* 25 (2020) 2815, <https://doi.org/10.3390/molecules25122815>.
- [24] E. Jasiukaitytė-Grojzdek, M. Huš, M. Grilc, B. Likozar, Acid-catalysed α -O-4 aryl-ether bond cleavage in methanol/(aqueous) ethanol: understanding depolymerisation of a lignin model compound during organosolv pretreatment, *Sci. Rep.* 10 (2020), <https://doi.org/10.1038/s41598-020-67787-9>.
- [25] D. Huang, R. Li, P. Xu, T. Li, R. Deng, S. Chen, Q. Zhang, The cornerstone of realizing lignin value-addition: Exploiting the native structure and properties of lignin by extraction methods, *Chem. Eng. J.* 402 (2020), 126237, <https://doi.org/10.1016/j.cej.2020.126237>.
- [26] L.I. Xu, J. Zhang, Q.-J. Zong, L.I. Wang, T. Xu, J. Gong, Z.-H. Liu, B.-Z. Li, Y.-J. Yuan, High-solid ethylenediamine pretreatment to fractionate new lignin streams from lignocellulosic biomass, *Chem. Eng. J.* 427 (2022) 130962.
- [27] P.J. Deuss, C.S. Lancefield, A. Narami, J.G. De Vries, N.J. Westwood, K. Barta, Phenolic acetals from lignins of varying compositions: Via iron(iii) triflate catalysed depolymerisation, *Green Chem.* 19 (2017) 2774–2782, <https://doi.org/10.1039/c7gc00195a>.
- [28] R. Parthasarathi, R.A. Romero, A. Redondo, S. Gnanakaran, Theoretical study of the remarkably diverse linkages in lignin, *J. Phys. Chem. Lett.* 2 (2011) 2660–2666, <https://doi.org/10.1021/jz201201q>.
- [29] S. Kim, S.C. Chmely, M.R. Nimlos, Y.J. Bomble, T.D. Foust, R.S. Paton, G. T. Beckham, Computational study of bond dissociation enthalpies for a large range of native and modified Lignins, *J. Phys. Chem. Lett.* 2 (2011) 2846–2852, <https://doi.org/10.1021/jz201182w>.
- [30] S. Wang, W.X. Li, Y.Q. Yang, X. Chen, J. Ma, C. Chen, L.P. Xiao, R.C. Sun, Unlocking structure-reactivity relationships for catalytic hydrogenolysis of lignin into phenolic monomers, *ChemSusChem* 13 (2020) 4548–4556, <https://doi.org/10.1002/cssc.202000785>.
- [31] M. Wang, J. Lu, X. Zhang, L. Li, H. Li, N. Luo, F. Wang, Two-step catalytic C-C bond oxidative cleavage process converts lignin models and extracts to aromatic acids, *ACS Catal.* 6 (2016) 6086–6090, <https://doi.org/10.1021/acscatal.6b02049>.
- [32] T. Renders, G. Van den Bossche, T. Vangeel, K. Van Aelst, B. Sels, Reductive catalytic fractionation: state of the art of the lignin-first biorefinery, *Curr. Opin. Biotechnol.* 56 (2019) 193–201, <https://doi.org/10.1016/j.copbio.2018.12.005>.
- [33] J.R. Meyer, H. Li, J. Zhang, M.B. Foston, Kinetics of secondary reactions affecting the organosolv lignin structure, *ChemSusChem* 13 (2020) 4557–4566, <https://doi.org/10.1002/cssc.202000942>.
- [34] D.M. Miles-Barrett, A.R. Neal, C. Hand, J.R.D. Montgomery, I. Panovic, O.S. Ojo, C.S. Lancefield, D.B. Cordes, A.M.Z. Slawin, T. Lebl, N.J. Westwood, The synthesis and analysis of lignin-bound Hibbert ketone structures in technical lignins, *Org. Biomol. Chem.* 14 (2016) 10023–10030, <https://doi.org/10.1039/c6ob01915c>.
- [35] C. Zhang, F. Wang, Catalytic Lignin Depolymerization to Aromatic Chemicals, *Acc. Chem. Res.* 53 (2) (2020) 470–484.
- [36] J. Gierer, Chemistry of delignification - Part 1: general concept and reactions during pulping, *Wood Sci. Technol.* 19 (1985) 289–312, <https://doi.org/10.1007/BF00350807>.
- [37] N. Li, Y. Li, C.G. Yoo, X. Yang, X. Lin, J. Ralph, X. Pan, An uncondensed lignin depolymerized in the solid state and isolated from lignocellulosic biomass: a mechanistic study, *Green Chem.* 20 (2018) 4224–4235, <https://doi.org/10.1039/c8gc00955h>.
- [38] V.M. Roberts, V. Stein, T. Reiner, A. Lemonidou, X. Li, J.A. Lercher, Towards quantitative catalytic lignin depolymerization, *Chem. - A Eur. J.* 17 (2011) 5939–5948, <https://doi.org/10.1002/chem.201002438>.
- [39] T.L.K. Yong, Y. Matsumura, Reaction kinetics of the lignin conversion in supercritical water, *Ind. Eng. Chem. Res.* 51 (2012) 11975–11988, <https://doi.org/10.1021/ie300921d>.
- [40] T. Faravelli, A. Frassoldati, G. Migliavacca, E. Ranzi, Detailed kinetic modeling of the thermal degradation of lignins, *Biomass and Bioenergy.* 34 (2010) 290–301, <https://doi.org/10.1016/j.biombioe.2009.10.018>.
- [41] S.O. Limarta, H. Kim, J.M. Ha, Y.K. Park, J. Jae, High-quality and phenolic monomer-rich bio-oil production from lignin in supercritical ethanol over synergistic Ru and Mg-Zr-oxide catalysts, *Chem. Eng. J.* 396 (2020), 125175, <https://doi.org/10.1016/j.cej.2020.125175>.
- [42] R. Shu, Y. Xu, L. Ma, Q. Zhang, C. Wang, Y. Chen, Controllable production of guaiacols and phenols from lignin depolymerization using Pd/C catalyst cooperated with metal chloride, *Chem. Eng. J.* 338 (2018) 457–464, <https://doi.org/10.1016/j.cej.2018.01.002>.
- [43] J. Sebastian, Y.W. Cheah, D. Bernin, D. Creaser, L. Olsson, The promoter and poison effects of the inorganic elements of kraft lignin during hydrotreatment over nimos catalyst, *Catalysts* 11 (2021) 1–15, <https://doi.org/10.3390/catal11080874>.
- [44] K. Van Aelst, E. Van Sinay, T. Vangeel, E. Cooreman, G. Van Den Bossche, T. Renders, J. Van Aelst, S. Van Den Bosch, B.F. Sels, Reductive catalytic fractionation of pine wood: elucidating and quantifying the molecular structures in the lignin oil, *Chem. Sci.* 11 (2020) 11498–11508, <https://doi.org/10.1039/d0sc04182c>.
- [45] Y. Liao, S.-F. Koelewijn, G. Van den Bossche, J. Van Aelst, S. Van den Bosch, T. Renders, K. Navare, T. Nicolaï, K. Van Aelst, M. Maesen, H. Matsushima, J. M. Thevelein, K. Van Acker, B. Lagrain, D. Verboeckend, B.F. Sels, A sustainable wood biorefinery for low-carbon footprint chemicals production, *Science* 367 (6484) (2020) 1385–1390.
- [46] R. Ma, M. Guo, X. Zhang, Recent advances in oxidative valorization of lignin, *Catal. Today* 302 (2018) 50–60, <https://doi.org/10.1016/j.cattod.2017.05.101>.
- [47] A. Bjelić, M. Grilc, S. Gyergyek, A. Kocjan, D. Makovec, B. Likozar, Catalytic hydrogenation, hydrodeoxygenation, and hydrocracking processes of a lignin monomer model compound eugenol over magnetic Ru/C–Fe₂O₃ and mechanistic reaction microkinetics, *Catalysts* 8 (10) (2018) 425.
- [48] X. Liu, Z. Jiang, S. Feng, H. Zhang, J. Li, C. Hu, Catalytic depolymerization of organosolv lignin to phenolic monomers and low molecular weight oligomers, *Fuel* 244 (2019) 247–257, <https://doi.org/10.1016/j.fuel.2019.01.117>.
- [49] A. Bjelić, M. Grilc, M. Huš, B. Likozar, Hydrogenation and hydrodeoxygenation of aromatic lignin monomers over Cu/C, Ni/C, Pd/C, Pt/C, Rh/C and Ru/C catalysts: mechanisms, reaction micro-kinetic modelling and quantitative

- structure-activity relationships, *Chem. Eng. J.* 359 (2019) 305–320, <https://doi.org/10.1016/j.cej.2018.11.107>.
- [50] T. Ren, S. You, M. Zhang, Y. Wang, W. Qi, R. Su, Z. He, Improved conversion efficiency of Lignin-to-Fuel conversion by limiting catalyst deactivation, *Chem. Eng. J.* 410 (2021), 128270, <https://doi.org/10.1016/j.cej.2020.128270>.
- [51] E. Terrell, L.D. Dellon, A. Dufour, E. Bartolomei, L.J. Broadbelt, M. Garcia-Perez, A review on lignin liquefaction: advanced characterization of structure and microkinetic modeling, *Ind. Eng. Chem. Res.* 59 (2020) 526–555, <https://doi.org/10.1021/acs.iecr.9b05744>.
- [52] N. Abad-Fernández, E. Pérez, Á. Martín, M.J. Cocero, Kraft lignin depolymerisation in sub- and supercritical water using ultrafast continuous reactors. Optimization and reaction kinetics, *J. Supercrit. Fluids.* 165 (2020) 104940.
- [53] D. Forchheim, J.R. Gasson, U. Hornung, A. Kruse, T. Barth, Modeling the lignin degradation kinetics in a ethanol/formic acid solvolysis approach. part 2. validation and transfer to variable conditions, *Ind. Eng. Chem. Res.* 51 (2012) 15053–15063, <https://doi.org/10.1021/ie3026407>.
- [54] A. Kloekhorst, H.J. Heeres, Catalytic hydrotreatment of alcell lignin using supported Ru, Pd, and Cu catalysts, *ACS Sustain. Chem. Eng.* 3 (2015) 1905–1914, <https://doi.org/10.1021/acssuschemeng.5b00041>.
- [55] A.J. Yanez, P. Natarajan, W. Li, R. Mabon, L.J. Broadbelt, Coupled structural and kinetic model of lignin fast pyrolysis, *Energy Fuels* 32 (2018) 1822–1830, <https://doi.org/10.1021/acs.energyfuels.7b03311>.
- [56] L. Dong, L. Lin, X. Han, X. Si, X. Liu, Y. Guo, F. Lu, S. Rudić, S.F. Parker, S. Yang, Y. Wang, Breaking the limit of lignin monomer production via cleavage of interunit carbon-carbon linkages, *Chemistry* 5 (2019) 1521–1536, <https://doi.org/10.1016/j.chempr.2019.03.007>.
- [57] X. Shen, Y. Xin, H. Liu, B. Han, Product-oriented direct cleavage of chemical linkages in lignin, *ChemSusChem* 13 (2020) 4367–4381, <https://doi.org/10.1002/cssc.202001025>.
- [58] D. Forchheim, U. Hornung, A. Kruse, T. Sutter, Kinetic modelling of hydrothermal lignin depolymerisation, *Waste and Biomass Valorization* 5 (2014) 985–994, <https://doi.org/10.1007/s12649-014-9307-6>.
- [59] V.N. Bui, D. Laurenti, P. Delichère, C. Geantet, Hydrodeoxygenation of guaiacol. Part II: support effect for CoMoS catalysts on HDO activity and selectivity, *Appl. Catal. B Environ.* 101 (2011) 246–255, <https://doi.org/10.1016/j.apcatb.2010.10.031>.
- [60] N. Joshi, A. Lawal, Hydrodeoxygenation of 4-propylguaiacol (2-methoxy-4-propylphenol) in a microreactor: performance and kinetic studies, *Ind. Eng. Chem. Res.* 52 (2013) 4049–4058, <https://doi.org/10.1021/ie400037y>.
- [61] A. Kloekhorst, Y. Shen, Y. Yie, M. Fang, H.J. Heeres, Catalytic hydrodeoxygenation and hydrocracking of Alcell® lignin in alcohol/formic acid mixtures using a Ru/C catalyst, *Biomass Bioenergy* 80 (2015) 147–161, <https://doi.org/10.1016/j.biombioe.2015.04.039>.
- [62] X. Huang, T.I. Korányi, M.D. Boot, E.J.M. Hensen, Catalytic depolymerization of lignin in supercritical ethanol, *ChemSusChem* 7 (2014) 2276–2288, <https://doi.org/10.1002/cssc.201402094>.
- [63] S.F. Koelewijn, C. Cooreman, T. Renders, C. Andecochea Saiz, S. Van Den Bosch, W. Schutyser, W. De Leger, M. Smet, P. Van Puyvelde, H. Witters, B. Van Der Bruggen, B.F. Sels, Promising bulk production of a potentially benign bisphenol A replacement from a hardwood lignin platform, *Green Chem.* 20 (2018) 1050–1058, <https://doi.org/10.1039/c7gc02989f>.
- [64] J.W. Thybaut, G.B. Marin, Single-event microKinetics: catalyst design for complex reaction networks, *J. Catal.* 308 (2013) 352–362, <https://doi.org/10.1016/j.jcat.2013.08.013>.
- [65] M. Sharifzadeh, M. Sadeqzadeh, M. Guo, T.N. Borhani, N.V.S.N. Murthy Konda, M.C. Garcia, L. Wang, J. Hallett, N. Shah, The multi-scale challenges of biomass fast pyrolysis and bio-oil upgrading: Review of the state of art and future research directions, *Prog. Energy Combust. Sci.* 71 (2019) 1–80, <https://doi.org/10.1016/j.pecc.2018.10.006>.
- [66] A. Sarvaramini, G.P. Assima, F. Larachi, Dry torrefaction of biomass – Torrefied products and torrefaction kinetics using the distributed activation energy model, *Chem. Eng. J.* 229 (2013) 498–507, <https://doi.org/10.1016/j.cej.2013.06.056>.
- [67] L.P. de Oliveira, D. Hudebine, D. Guillaume, J.J. Verstraete, J.F. Joly, A Review of kinetic modeling methodologies for complex processes, *Oil Gas Sci. Technol.* 71 (3) (2016) 45.
- [68] C. Zhu, J.-P. Cao, T. Xie, X.-Y. Zhao, X. Cui, Z.-X. Guo, W.-Z. Shen, J. Bai, X.-Y. Wei, Comparison of kinetics and activity of Ni-based catalysts for benzyl phenyl ether catalytic hydrogenolysis, *Energy Technol.* 7 (3) (2019) 1800694.
- [69] B. Gomez-Monedero, J. Faria, F. Bimbela, M.P. Ruiz, Catalytic hydroprocessing of lignin β -O-4 ether bond model compound phenethyl phenyl ether over ruthenium catalysts, *Biomass Convers. Biorefinery* 7 (2017) 385–398, <https://doi.org/10.1007/s13399-017-0275-5>.
- [70] B. Zhang, H.J. Huang, S. Ramaswamy, Reaction kinetics of the hydrothermal treatment of lignin, *Appl. Biochem. Biotechnol.* 147 (2008) 119–131, <https://doi.org/10.1007/s12010-007-8070-6>.
- [71] R. Obeid, D.M. Lewis, N. Smith, T. Hall, P. Van Eyk, Reaction kinetics and characterization of species in renewable crude from hydrothermal liquefaction of mixtures of polymer compounds to represent organic fractions of biomass feedstocks, *Energy Fuels* 34 (2020) 419–429, <https://doi.org/10.1021/acs.energyfuels.9b02936>.
- [72] J.J. Bernhardt, B. Rößiger, T. Hahn, D. Pufky-Heinrich, Kinetic modeling of the continuous hydrothermal base catalyzed depolymerization of pine wood based kraft lignin in pilot scale, *Ind. Crops Prod.* 159 (2021) 113119.
- [73] E.M. Anderson, M.L. Stone, M.J. Hülsey, G.T. Beckham, Y. Román-Leshkov, Kinetic studies of lignin solvolysis and reduction by reductive catalytic fractionation decoupled in flow-through reactors, *ACS Sustain. Chem. Eng.* 6 (2018) 7951–7959, <https://doi.org/10.1021/acssuschemeng.8b01256>.
- [74] E. Jasiukaitytė-Grojzdek, M. Hus, M. Grilc, B. Likozar, Acid-Catalyzed α -O-4 Aryl-Ether Cleavage Mechanisms in (Aqueous) γ -Valerolactone: Catalytic Depolymerization Reactions of Lignin Model Compound during Organosolv Pretreatment, *ACS Sustain. Chem. Eng.* 8 (2020) 17475–17486, <https://doi.org/10.1021/acssuschemeng.0c06099>.
- [75] N. Bijok, J. Fiskari, R.R. Gustafson, V. Alopaeus, Modelling the kraft pulping process on a fibre scale by considering the intrinsic heterogeneous nature of the lignocellulosic feedstock, *Chem. Eng. J.* 438 (2022) 135548.
- [76] J.P.F. Simão, M.G.V.S. Carvalho, C.M.S.G. Baptista, Heterogeneous studies in pulping of wood: Modelling mass transfer of dissolved lignin, *Chem. Eng. J.* 170 (2011) 264–269, <https://doi.org/10.1016/j.cej.2011.03.046>.
- [77] J. Köcheremann, J. Mühlberg, M. Klemm, Kinetics of Hydrothermal Furfural Production from Organosolv Hemicellulose and d -Xylose, *Ind. Eng. Chem. Res.* 57 (2018) 14417–14427, <https://doi.org/10.1021/acs.iecr.8b03402>.
- [78] J. Köcheremann, J. Schreiber, M. Klemm, Conversion of d -Xylose and hemicellulose in water/ethanol mixtures, *ACS Sustain. Chem. Eng.* 7 (2019) 12323–12330, <https://doi.org/10.1021/acssuschemeng.9b01697>.
- [79] F.E. Massoth, P. Politzer, M.C. Concha, J.S. Murray, J. Jakowski, J. Simons, Catalytic hydrodeoxygenation of methyl-substituted phenols: correlations of kinetic parameters with molecular properties, *J. Phys. Chem. B* 110 (2006) 14283–14291, <https://doi.org/10.1021/jp057332g>.
- [80] V.N. Bui, D. Laurenti, P. Afanasiev, C. Geantet, Hydrodeoxygenation of guaiacol with CoMo catalysts. Part I: promoting effect of cobalt on HDO selectivity and activity, *Appl. Catal. B Environ.* 101 (2011) 239–245, <https://doi.org/10.1016/j.apcatb.2010.10.025>.
- [81] S. Tieuli, P. Mäki-Arvela, M. Peurla, K. Eränen, J. Wärnä, G. Cruciani, F. Menegazzo, D.Y. Murzin, M. Signoretto, Hydrodeoxygenation of isoeugenol over Ni-SBA-15: kinetics and modelling, *Appl. Catal. A Gen.* 580 (2019) 1–10, <https://doi.org/10.1016/j.apcata.2019.04.028>.
- [82] J. Zhang, B. Sudduth, J. Sun, Y. Wang, Hydrodeoxygenation of lignin-derived aromatic oxygenates over Pd-Fe bimetallic catalyst: a mechanistic study of direct C-O Bond cleavage and direct ring hydrogenation, *Catal. Letters.* 151 (4) (2021) 932–939.
- [83] R. Van De Vijver, N.M. Vandewiele, P.L. Bhoorasingh, B.L. Slakman, F. S. Khanshan, H.H. Carstensen, M.F. Reyniers, G.B. Marin, R.H. West, K.M. Van Geem, Automatic mechanism and kinetic model generation for gas- And solution-phase processes: a perspective on best practices, recent advances, and future challenges, *Int. J. Chem. Kinet.* 47 (2015) 199–231, <https://doi.org/10.1002/kin.20902>.
- [84] B.D. Mar, H.W. Qi, F. Liu, H.J. Kulik, Ab initio screening approach for the discovery of lignin polymer breaking pathways, *J. Phys. Chem. A* 119 (2015) 6551–6562, <https://doi.org/10.1021/acs.jpca.5b03503>.
- [85] M. Grilc, B. Likozar, J. Levec, Kinetic model of homogeneous lignocellulosic biomass solvolysis in glycerol and imidazolium-based ionic liquids with subsequent heterogeneous hydrodeoxygenation over NiMo/Al₂O₃ catalyst, *Catal. Today* 256 (2015) 302–314, <https://doi.org/10.1016/j.cattod.2015.02.034>.
- [86] M.B. Pecha, J.I.M. Arbelaez, M. Garcia-Perez, F. Chejne, P.N. Ciesielski, Progress in understanding the four dominant intra-particle phenomena of lignocellulose pyrolysis: Chemical reactions, heat transfer, mass transfer, and phase change, *R. Soc. Chem.* 21 (11) (2019) 2868–2898.
- [87] X. Wei, W. Li, Q. Liu, W. Sun, S. Liu, S. Li, H. Wei, L. Ma, Pore-scale investigation on multiphase reactive transport for the conversion of levulinic acid to γ -valerolactone with Ru/C catalyst, *Chem. Eng. J.* 427 (2022) 130917.
- [88] C. Sievers, S.L. Scott, Y. Noda, L. Qi, E.M. Albuquerque, R.M. Rioux, Phenomena affecting catalytic reactions at solid–Liquid interfaces, *ACS Catal.* 6 (2016) 8286–8307, <https://doi.org/10.1021/acscatal.6b02532>.
- [89] M.D. Argyle, C.H. Bartholomew, Heterogeneous catalyst deactivation and regeneration: a review, *Catalysts* 5 (2015) 145–269, <https://doi.org/10.3390/catal5010145>.
- [90] P.N. Ciesielski, M.B. Pecha, N.E. Thornburg, M.F. Crowley, X. Gao, O. Oyedeji, H. Sitarman, N. Brunhart-Lupo, Bridging scales in bioenergy and catalysis: a review of mesoscale modeling applications, methods, and future directions, *Energy Fuels* 35 (2021) 14382–14400, <https://doi.org/10.1021/acs.energyfuels.1c02163>.
- [91] V.S. Bharadwaj, M.B. Pecha, L. Bu, V.L. Dagle, R.A. Dagle, P.N. Ciesielski, Multi-scale simulation of reaction, transport and deactivation in a SBA-16 supported catalyst for the conversion of ethanol to butadiene, *Catal. Today* 338 (2019) 141–151, <https://doi.org/10.1016/j.cattod.2019.05.042>.
- [92] N.E. Thornburg, M.B. Pecha, D.G. Brandner, M.L. Reed, J.V. Vermaas, W. N. E. Michener, R. Katahira, T.B. Vinzant, T.D. Foust, B.S. Donohoe, Y. Román-Leshkov, P.N. Ciesielski, G.T. Beckham, Mesoscale reaction-diffusion phenomena governing lignin-first biomass fractionation, *ChemSusChem* 13 (2020) 4495–4509, <https://doi.org/10.1002/cssc.202000558>.
- [93] N.E. Thornburg, R.M. Ness, M.F. Crowley, L. Bu, M.B. Pecha, F.L.E. Usseglio-Viretta, V.S. Bharadwaj, Y. Li, X. Chen, D.A. Sievers, E.J. Wolfrum, M.G. Resch, P. N. Ciesielski, Mass transport limitations and kinetic consequences of corn stover deacetylation, *Front. Energy Res.* 10 (2022) 1–15, <https://doi.org/10.3389/ferg.2022.841169>.
- [94] J.S. Luterbacher, J.Y. Parlange, L.P. Walker, A pore-hindered diffusion and reaction model can help explain the importance of pore size distribution in enzymatic hydrolysis of biomass, *Biotechnol. Bioeng.* 110 (2013) 127–136, <https://doi.org/10.1002/bit.24614>.

- [195] J. Liu, W. Qu, Y. Xie, B. Zhu, T. Wang, X. Bai, X. Wang, Thermal conductivity and annealing effect on structure of lignin-based microscale carbon fibers, *Carbon N. Y.* 121 (2017) 35–47, <https://doi.org/10.1016/j.carbon.2017.05.066>.
- [196] D.L. Pyle, C.A. Zaror, Heat transfer and kinetics in the low temperature pyrolysis of solids, *Chem. Eng. Sci.* 39 (1984) 147–158, [https://doi.org/10.1016/0009-2509\(84\)80140-2](https://doi.org/10.1016/0009-2509(84)80140-2).
- [197] A. Dufour, B. Ouartassi, R. Bounaceur, A. Zoulalian, Modelling intra-particle phenomena of biomass pyrolysis, *Chem. Eng. Res. Des.* 89 (2011) 2136–2146, <https://doi.org/10.1016/j.cherd.2011.01.005>.
- [198] Q. Xiong, S.C. Kong, High-resolution particle-scale simulation of biomass pyrolysis, *ACS Sustain. Chem. Eng.* 4 (2016) 5456–5461, <https://doi.org/10.1021/acssuschemeng.6b01020>.
- [199] P.N. Ciesielski, M.F. Crowley, M.R. Nimlos, A.W. Sanders, G.M. Wiggins, D. Robichaud, B.S. Donohoe, T.D. Foust, Biomass particle models with realistic morphology and resolved microstructure for simulations of intraparticle transport phenomena, *Energy Fuels* 29 (2015) 242–254, <https://doi.org/10.1021/ef502204v>.
- [100] X.i. Gao, L. Lu, M. Shahnam, W.A. Rogers, K. Smith, K. Gaston, D. Robichaud, M. Brennan Pecha, M. Crowley, P.N. Ciesielski, P. Debiagi, T. Faravelli, G. Wiggins, C.E.A. Finney, J.E. Parks, Assessment of a detailed biomass pyrolysis kinetic scheme in multiscale simulations of a single-particle pyrolyzer and a pilot-scale entrained flow pyrolyzer, *Chem. Eng. J.* 418 (2021) 129347.
- [101] M.B. Pecha, M. Garcia-Perez, T.D. Foust, P.N. Ciesielski, Estimation of heat transfer coefficients for biomass particles by direct numerical simulation using microstructured particle models in the laminar regime, *ACS Sustain. Chem. Eng.* 5 (2017) 1046–1053, <https://doi.org/10.1021/acssuschemeng.6b02341>.
- [102] J.D. Jackson, Fluid flow and convective heat transfer to fluids at supercritical pressure, *Nucl. Eng. Des.* 264 (2013) 24–40, <https://doi.org/10.1016/j.nucengdes.2012.09.040>.
- [103] X. Cheng, B. Kuang, Y.H. Yang, Numerical analysis of heat transfer in supercritical water cooled flow channels, *Nucl. Eng. Des.* 237 (2007) 240–252, <https://doi.org/10.1016/j.nucengdes.2006.06.011>.
- [104] J. Quesada-Medina, F.J. López-Cremades, P. Olivares-Carrillo, Organosolv extraction of lignin from hydrolyzed almond shells and application of the δ -value theory, *Bioresour. Technol.* 101 (2010) 8252–8260, <https://doi.org/10.1016/j.biortech.2010.06.011>.
- [105] Y. Ye, Y. Liu, J. Chang, Application of solubility parameter theory to organosolv extraction of lignin from enzymatically hydrolyzed cornstalks, *BioResources* 9 (2014) 3417–3427, <https://doi.org/10.15376/biores.9.2.3417-3427>.
- [106] Y. Ni, Q. Hu, Alcell® lignin solubility in ethanol–water mixtures, *J. Appl. Polym. Sci.* 57 (1995) 1441–1446, <https://doi.org/10.1002/app.1995.070571203>.
- [107] W.M. Goldmann, J. Ahola, M. Mikola, J. Tanskanen, Solubility and fractionation of Indulin AT kraft lignin in ethanol-water media, *Sep. Purif. Technol.* 209 (2019) 826–832, <https://doi.org/10.1016/j.seppur.2018.06.054>.
- [108] B. Soares, D.J.P. Tavares, J.L. Amaral, A.J.D. Silvestre, C.S.R. Freire, J.A. P. Coutinho, Enhanced solubility of lignin monomeric model compounds and technical lignins in aqueous solutions of deep eutectic solvents, *ACS Sustain. Chem. Eng.* 5 (2017) 4056–4065, <https://doi.org/10.1021/acssuschemeng.7b00053>.
- [109] F.H.B. Sosa, D.O. Abranches, A.M. Da Costa Lopes, J.A.P. Coutinho, M.C. Da Costa, Kraft lignin solubility and its chemical modification in deep eutectic solvents, *ACS Sustain. Chem. Eng.* 8 (2020) 18577–18589, <https://doi.org/10.1021/acssuschemeng.0c06655>.
- [110] G. Ivaniš, L. Fele Žilnik, B. Likozar, M. Grilc, Hydrogen solubility in bio-based furfural and furfuryl alcohol at elevated temperatures and pressures relevant for hydrodeoxygenation, *Fuel* 290 (2021) 1–11, <https://doi.org/10.1016/j.fuel.2020.120021>.
- [111] L.F. Žilnik, M. Grilc, B. Likozar, Hydrogen solubility equilibria in bio-based Guaiacol or Levulinic acid/water mixture as lignin or cellulose depolymerization model solutions, *Fluid Phase Equilib.* 546 (2021) 113115.
- [112] E. Brunner, Solubility of hydrogen in 10 organic solvents at 298.15, 323.15, and 373.15 K, *J. Chem. Eng. Data* 30 (1985) 269–273, <https://doi.org/10.1021/jc00041a010>.
- [113] J.M. Shaw, A correlation for hydrogen solubility in alicyclic and aromatic solvents, *Can. J. Chem. Eng.* 65 (1987) 293–298, <https://doi.org/10.1002/cjce.5450650215>.
- [114] M. Herskowitz, J. Wlsnlak, L. Skladman, Hydrogen solubility in organic liquids, *J. Chem. Eng. Data* 28 (1983) 164–166, <https://doi.org/10.1021/jc00032a009>.